Cyclic Hexapeptides and Chimeric Peptides as Mimics of Tendamistat

Felicia A. Etzkorn, Tao Guo, Mark A. Lipton, Steven D. Goldberg, and Paul A. Bartlett*

Contribution from the Department of Chemistry, University of California, Berkeley, California 94720-1460

Received May 3, 1994[⊗]

Abstract: We describe the design and evaluation of structural mimics of tendamistat, a 74-residue proteinaceous inhibitor of α-amylase. Cyclic hexapeptides were designed in which the sequence Trp-Arg-Tyr is constrained to the $i + 1$ to $i + 3$ positions of a type I β-turn; these compounds inhibit α-amylase with K_i values of 14−32 μM, significantly more tightly than related linear tri- and hexapeptides. Incorporation of the bicyclic Nagai−Sato type II β-turn mimic opposite the Trp-Arg-Tyr sequence in a chimeric molecule leads to a weaker inhibitor. NMR studies indicate that the desired β-turn conformation is adopted by the cyclic hexapeptides but not by the chimeric molecule, supporting the interpretation that the former are indeed acting as small molecule mimics of tendamistat.

There are a number of ways in which structural information can be used in the design of an enzyme inhibitor or receptor ligand. Perhaps the most obvious opportunity is presented by a structure of the protein binding site itself. This increasingly common circumstance has stimulated the development of several strategies for *de novo* design.[1−8] The three-dimensional structure of a naturally-occurring ligand for the binding site also presents an opportunity for structure-based design. Indeed, these opportunities may be more common than the former, since the structures or conformations of soluble ligands are often more accessible than the structures of macromolecular, usually membrane-associated receptors.[9] Although a naturally-occurring ligand may be too large or unstable to serve as a practical lead in an analog study, it still represents one solution to the three-dimensional design problem. In these circumstances, a goal of structure-based design is to discover a *mimic* of the natural ligand, a smaller, preferably nonpeptidic molecule that retains some of the structural and electronic features of the lead structure, and thus emulates some of its binding characteristics.

Tendamistat, a protein of 74 residues that inhibits α-amylase, provides a useful system for the development of such an approach. This protein from *Streptomyces tendae*[10] was one of the first biological macromolecules solved independently by X-ray crystallography[11] and 2D NMR techniques.[12] It is a potent inhibitor of porcine pancreatic α-amylase, with an inhibition constant K_i = 0.2 nM.[10] Homology with other proteinaceous α-amylase inhibitors,[13] as well as UV difference spectroscopy studies,[14] suggested that the surface loop comprised of ^{18}Trp-^{19}Arg-^{20}Tyr is a key element in the interaction of tendamistat with the enzyme. Preliminary studies on the structure of the complex between tendamistat and α-amylase have confirmed that this "active loop" lies at the center of the interacting surface of tendamistat.[15]

In crystals of tendamistat itself, the ^{18}Trp-^{19}Arg-^{20}Tyr residues occupy the $i + 1$ to $i + 3$ positions of a slightly distorted type I β-turn, with the ^{19}Arg side chain sandwiched between the adjacent aromatic rings (Figure 1a).[11] Presumably, the cationic guanidinium and the hydrogen-bonding phenol and indole moieties interact with complementary groups in the enzyme active site, with the hydrophobic regions contributing to binding as well. The structures of tendamistat in solution and in the crystal are similar with respect to the conformations of the peptide backbone and the interior peptide side chains, although the NMR studies indicate considerable flexibility for the side chains on the surface of the protein.[16] Both the NMR and crystal structures suggest some backbone flexibility in the region of the active loop,[16] although the preliminary structural information on the tendamistat−α-amylase complex indicates that the bound conformation of this loop is close to that in the crystal structure of tendamistat alone.[15]

Tendamistat is an attractive target for mimic design because of the nature of the structural information available, and because it presents an opportunity to explore the question of whether a small molecule structural mimic can emulate the binding characteristics of a much larger protein inhibitor. There is considerable interest in mimics of β-turn structures,[17−19] since they have been implicated as recognition elements in a variety

[⊗] Abstract published in *Advance ACS Abstracts,* November 1, 1994.

(1) Richards, W. G. *Pure Appl. Chem.* **1993**, *65*, 231−234.
(2) Kuntz, I. D. *Science* **1992**, *257*, 1078−1082.
(3) Walkinshaw, M. D. *Med. Res. Rev.* **1992**, *12*, 317−372.
(4) Martin, Y. C.; Bures, M. G.; Danaher, E. A.; DeLazzer, J.; Lico, I.; Pavlik, P. A. *J. Comput.-Aided Mol. Des.* **1993**, *7*, 83−102.
(5) Kempf, D. J.; Norbeck, D. W.; Codacovi, L.; Wang, X. C.; Kohlbrenner, W. E.; Wideburg, N. E.; Paul, D. A.; Knigge, M. F.; Vasavanonda, S.; Craig-Kennard, A.; Saldivar, A.; Rosenbrook, W., Jr.; Clement, J. J.; Plattner, J. J.; Erickson, J. *J. Med. Chem.* **1990**, *33*, 2687−2689.
(6) DesJarlais, R. L.; Seibel, G. L.; Kuntz, I. D.; Furth, P. S.; Alvarez, J. C.; Ortiz de Montellano, P. R.; DeCamp, D. L.; Babé, L. M.; Craik, C. S. *Proc. Natl. Acad. Sci. U.S.A.* **1990**, *87*, 6644−6648.
(7) Appelt, K.; Bacquet, R. J.; Bartlett, C. A.; Booth, C. L. J.; Freer, S. T.; Fuhry, M. M.; Gehring, M. R.; Herrmann, S. M.; Howland, E. F. *J. Med. Chem.* **1991**, *34*, 1925−1934.
(8) Goodford, P. J. *J. Med. Chem.* **1985**, *28*, 849−857.
(9) Erickson, J. W.; Fesik, S. W. *Annu. Rep. Med. Chem.* **1992**, *27*, 271−289.
(10) Vértesy, L.; Oeding, V.; Bender, R.; Zepf, K.; Nesemann, G. *Eur. J. Biochem.* **1984**, *141*, 505−512.
(11) Pflugrath, J. W.; Wiegand, G.; Huber, R.; Vértesy, L. *J. Mol. Biol.* **1986**, *189*, 383−386.
(12) Kline, A. D.; Braun, W.; Wüthrich, K. *J. Mol. Biol.* **1986**, *189*, 367−382.
(13) Hofmann, O.; Vértesy, L.; Braunitzer, G. *Biol. Chem. Hoppe-Seyler* **1985**, *366*, 1161−1168.
(14) Goto, A.; Matsui, Y.; Ohyama, K.; Arai, M.; Murao, S. *Agric. Biol. Chem.* **1985**, *49*, 435−439.
(15) Huber, R.; Epp, O.; Wiegand, G. Personal communication.
(16) Billeter, M.; Kline, A. D.; Braun, W.; Huber, R.; Wüthrich, K. *J. Mol. Biol.* **1986**, *206*, 677−687.
(17) Ball, J. B.; Alewood, P. F. *J. Mol. Recognit.* **1990**, *3*, 55−64.

0002-7863/94/1516-10412$04.50/0

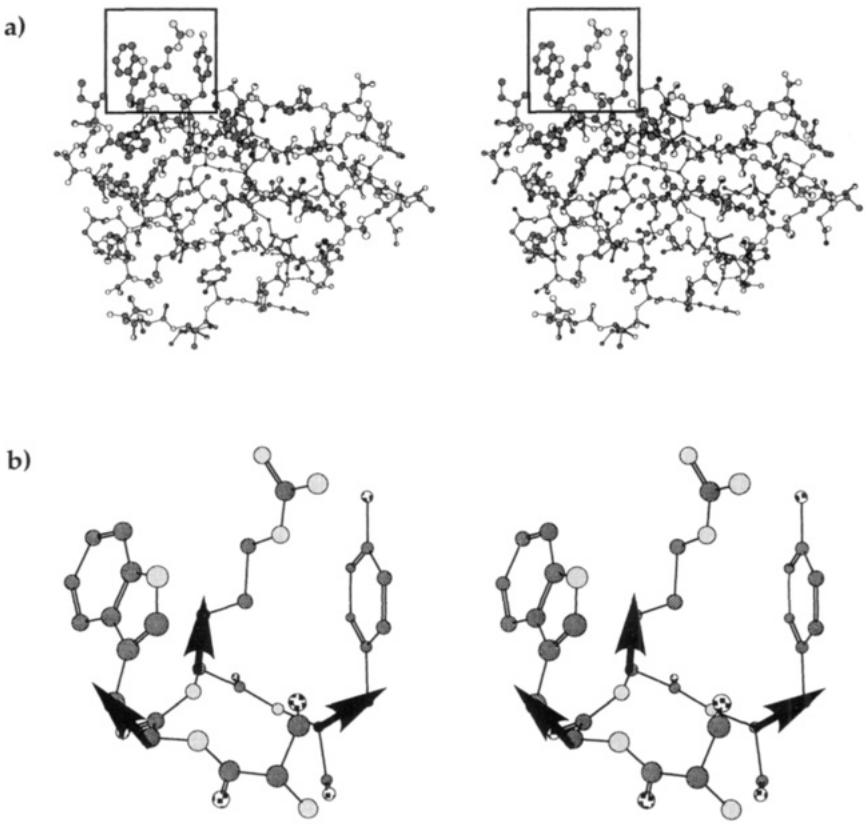

Figure 1. (a) Stereoview of the active loop region of tendamistat. (b) Vectors defined from Cα−Cβ bonds of residues 18−20 of tendamistat.

of biological interactions.[20−23] Moreover, as a peptide, tendamistat presents a completely different collection of functional groups than found in the polysaccharides the enzyme active site evolved to bind. A mimic of tendamistat could therefore be an inhibitor of α-amylase designed in a distinctively different manner from the known substrate or transition-state analogs.[24] While we did not expect that small molecule mimics would attain the same affinity as tendamistat, because of its large interaction surface with α-amylase, this system offered an opportunity to evaluate the template approach to mimic design and the effect of conformational restriction on affinity. In this paper, we describe our first steps toward these objectives.

Design Concepts

In devising a mimic of the active loop of tendamistat, we distinguished between the functional groups at the ends of the side chains, which interact directly with the enzyme, and the peptide backbone, which serves as a scaffold for these side chains. The backbone of the active loop of tendamistat is not exposed, suggesting that its major role is to position and orient the side chains appropriately. If the bound conformation of tendamistat were known in detail, we could devise a mimic that positions an indole ring, a guanidinium group, and a phenolic hydroxyl in the same relative orientation. Without this information, we believed it more prudent to focus on the peptide backbone and seek an alternative structure to serve as a scaffold. Although there is flexibility in the backbone, we had more confidence that this element of the tendamistat crystal structure would be preserved in the bound conformation. Accordingly, we sought ways to replace the peptide backbone of the active loop of tendamistat, as well as approaches that would constrain a peptide in the desired type I β-turn conformation.

Aside from locating the Cα atoms of the three residues a certain distance apart, the peptide backbone also orients the Cα−Cβ bonds of the side-chains in a specific way (Figure 1b). Mimicking the *vector* relationship of these bonds, in contrast to simply reproducing the *Cartesian* relationship of the Cα atoms, is an important concept in structure-based design, since the necessary side chain conformation cannot be assured otherwise. Recognition of this design concept provided the foundation for the program CAVEAT,[25,26] which performs vector-based searches of three-dimensional databases to assist in identifying useful templates or structural fragments.

Two approaches led to the identification of specific cyclic hexapeptides as potential templates for the tendamistat active loop. Independent modeling studies on somatostatin analogs resulted in the serendipitous observation that a portion of cyclo-[D-Pro-Phe-Thr-Phe-Trp-Phe], **1**,[27] can be superimposed on the tendamistat β-turn backbone (Figure 2). Subsequently, after the development of CAVEAT, both this peptide and cyclo[Phe-D-Leu-Gly-Phe-Leu-Gly], **2**,[28] were identified as matching the Cα−Cβ vectors of all four residues in the tendamistat β-turn (^{17}Ser-^{18}Trp-^{19}Arg-^{20}Tyr).

(18) Genin, M. J.; Ojala, W. H.; Gleason, W. B.; Johnson, R. L. *J. Org. Chem.* **1993**, *58*, 2334−2337.
(19) Hoelzemann, G. *Kontakte (Darmstadt)* **1991**, *1*, 3−12.
(20) Tainer, J. A.; Getzoff, E. D.; Alexander, H.; Houghton, R. A.; Olson, A. J.; Lerner, R. A.; Hendrickson, W. A. *Nature* **1984**, *312*, 127−134.
(21) Small, D.; Chou, P. Y.; Fasman, G. D. *Biochem. Biophys. Res. Commun.* **1977**, *79*, 341−346.
(22) Kahn, M.; Nakanishi, H.; Chrusciel, R. A.; Fitzpatrick, D.; Johnson, M. E. *J. Med. Chem.* **1991**, *34*, 3395−3399.
(23) Kyle, D. J.; Green, L. M.; Blake, P. R.; Smithwick, D.; Summers, M. F. *Pept. Res.* **1992**, *5*, 206−209.
(24) Laszlo, E.; Hollo, J.; Hoschke, A.; Sarosi, G. *Carbohydr. Res.* **1978**, *61*, 387−394.
(25) Bartlett, P. A.; Shea, G. T.; Telfer, S. J.; Waterman, S. In *Molecular Recognition: Chemical and Biological Problems*; Roberts, S. M., Ed.; Royal Society of Chemistry: London, 1989; pp 182−196.
(26) Lauri, G.; Bartlett, P. A. *J. Comput.-Aided Mol. Des.* **1994**, *8*, 51−66.
(27) Kessler, H.; Bats, J. W.; Griesinger, C.; Koll, S.; Will, M.; Wagner, K. *J. Am. Chem. Soc.* **1988**, *110*, 1033−1049.
(28) Barnes, C. L.; van der Helm, D. *Acta Crystallogr., Sect. B* **1982**, *38*, 2589.

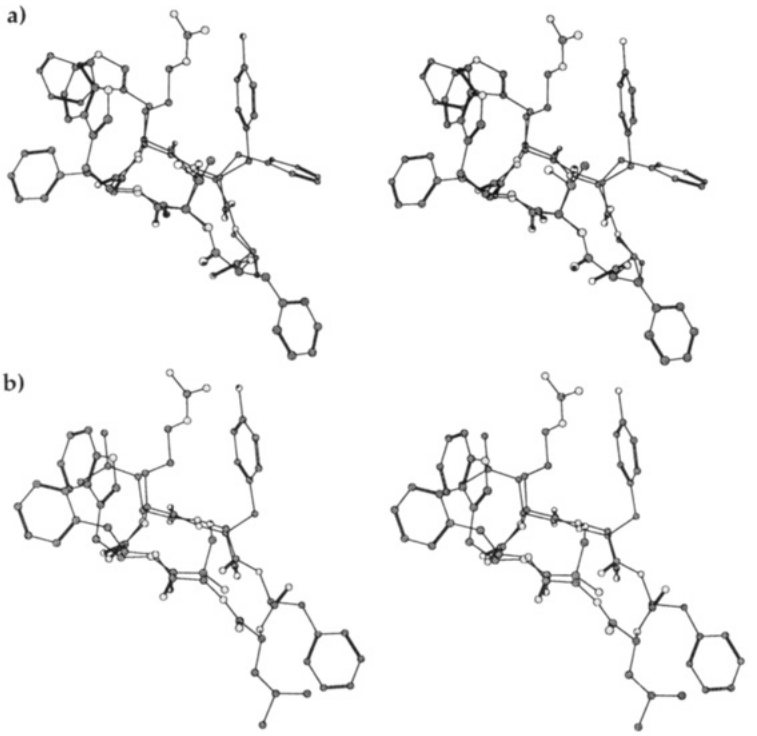

Figure 2. (a) Superposition of cyclo[D-PFTFWF] on residues 17−20 of tendamistat (rms deviation 0.40 Å for the eight-atom match of Cα and Cβ carbons). (b) Superposition of cyclo[F-D-LGFLG] (rms deviation 0.42 Å for six-atom match).

Both of these peptides adopt the dual β-turn structure that is commonly observed for cyclic hexapeptides.[29,30] In **2**, the type I β-turn of Phe-Leu is opposite a type II turn between Phe-D-Leu; in contrast, the type I β-turn of Phe-Trp in **1** is induced by a type II′ β-turn at D-Pro-Phe. In a study of the conformation and activity of a number of somatostatin analogs related to **1**, Kessler et al. found that the threonine residue could be replaced with alanine without affecting the biological activity or conformation.[31] Thus, cyclo[D-Pro-Phe-Ala-Trp-Arg-Tyr], **3**, emerged as one design for a potential tendamistat mimic.

In a second design, cyclo[D-Pro-Phe-Ser-Trp-Arg-Tyr], **4**, alanine is replaced with serine, since this residue at position 17 in tendamistat is also highly conserved in related inhibitors.[13] The crystal structure of tendamistat suggests that the side chain hydroxyl of ^{17}Ser engages in a hydrogen bond across the β-turn, perhaps stabilizing a specific conformation for the turn.

The well-precedented induction of specific peptide conformations by appropriate placement of D-amino acid residues or of nonpeptide templates[32−34] suggested a variation on the cyclic hexapeptide motif for mimicking tendamistat, namely, design of a chimeric molecule in which the desired type I β-turn would be induced in Xaa-Trp-Arg-Tyr by a rigid, nonpeptidic moiety. Again, we arrived at the selection of such a unit by two independent routes. The bicyclic "β-turn dipeptide" of Nagai and Sato (**5**, L-BTD) was designed to mimic a type II′ β-turn; it is an effective replacement for the D-Phe-L-Pro residues in gramicidin S, which are known to adopt the type II′ conformation.[35] A similar 6,5-ring system was identified in a CAVEAT search for a cyclic system to bridge two bonds in a typical β-sheet structure. The bicyclic lactam FIVXUD,[36] **6**, was retrieved from the Cambridge Structural Database[37] because two of the substituent bonds overlapped with the vectors defined for the CAVEAT search. From this hit, simplification of the structure and synthetic considerations rapidly melded the design with that of L-BTD. The bicyclic unit was synthesized in both enantiomeric forms (L-BTD and D-BTD) and incorporated into the cyclic chimeras D-**7**, L-**7**, and L-**8**.

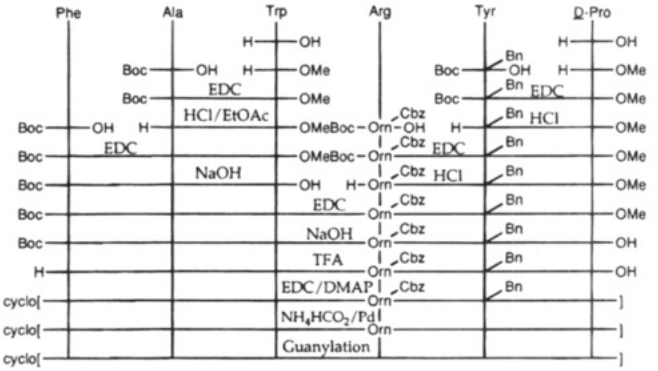

Figure 3. Synthesis of cyclo[D-PFAWRY], **3**.

Synthesis

The linear peptide precursors to **3** and **4** were assembled by solution-phase synthesis with benzylic side chain protection and Boc protection for the α-amino groups (Figure 3). Ethyl[(*N*,*N*-dimethylamino)propyl]carbodiimide (EDC) was used as the coupling agent in the presence of hydroxybenzotriazole (HOBT) to prepare the protected peptides.[38] Boc deprotections were

(29) Gierasch, L. M.; Deber, C. M.; Madison, V.; Niu, C.-H.; Blout, E. R. *Biochemistry* **1981**, *20*, 4730−4738.
(30) Bean, J. W.; Kopple, K. D.; Peishoff, C. E. *J. Am. Chem. Soc.* **1992**, *114*, 5328−5334.
(31) Kessler, H.; Gemmecker, G.; Haupt, A.; Klein, M.; Wagner, K.; Will, M. *Tetrahedron* **1988**, *44*, 745−759.
(32) Huffman, W. F.; Callahan, J. F.; Codd, E. E.; Eggleston, D. S.; Lemieux, C.; Newlander, K. A.; Schiller, P. W.; Takata, D. T.; Walker, R. F. *Synthetic Peptides: Approaches to Biological Problems;* Alan R. Liss, Inc.: New York, 1989; pp 257−266.
(33) Kemp, D. S. *Trends Biotechnol.* **1990**, *8*, 249−255.
(34) Diaz, H.; Tsang, K. Y.; Choo, D.; Espina, J. R.; Kelly, J. W. *J. Am. Chem. Soc.* **1993**, *115*, 3790−3791.
(35) Sato, K.; Nagai, U. *J. Chem. Soc., Perkin Trans. 1* **1986**, 1231−1236.
(36) Austin, G. N.; Baird, P. D.; Fleet, G. W. J.; Peach, J. M.; Smith, P. W.; Watkin, D. J. *Tetrahedron* **1987**, *43*, 3095−3108.
(37) Allen, F. H.; Kennard, O.; Taylor, R. *Acc. Chem. Res.* **1983**, *16*, 146−153.

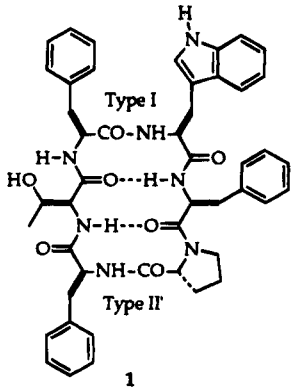

1

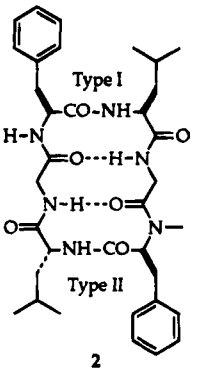

2

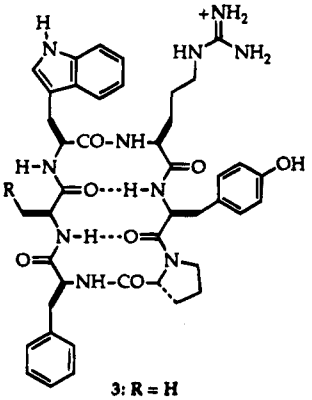

3: R = H
4: R = OH

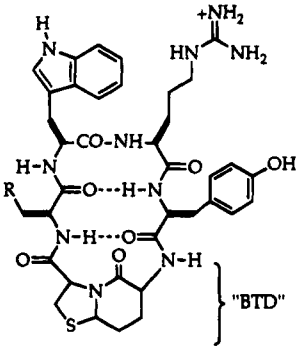

D-7: R = H, D-BTD
L-7: R = H, L-BTD
L-8: R = OH, L-BTD

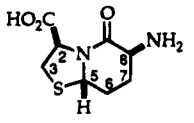

5

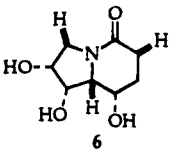

6

carried out with HCl in ethyl acetate to avoid trifluoroacetylation[39] of the products.

A number of reagents were evaluated for cyclization of the linear, protected hexapeptides, including the peptide coupling reagents diphenylphosphoryl azide (DPPA),[40] 1,1′-carbonylbis(3-methylimidazolium) triflate,[41] bis(2-oxo-3-oxazolidinyl)phosphinic chloride,[42] and (benzotriazol-1-yloxy)tris(dimethylamino)phosphonium hexafluorophosphate.[43] However, the transformation was accomplished most efficiently with EDC in the presence of 4-(dimethylamino)pyridine (DMAP), in a manner analogous to the macrolactonization method of Keck et al.[44] Slow addition of end-deprotected hexapeptide to a solution of EDC, DMAP, and DMAP·HCl in refluxing, alcohol-free $CHCl_3$ resulted in 12−15% yields of the desired cyclic products after HPLC purification.

We were unable to effect complete removal of the benzyl and carbobenzoxy side chain protecting groups under standard hydrogenolysis conditions with Pd/C. The protecting groups were removed quantitatively by catalytic transfer hydrogenation with ammonium formate over palladium under N_2.[45] Conversion of the ornithine residue to arginine was readily achieved using 3,5-dimethylpyrazole-1-carboxamidine nitrate as the guanidation reagent[46] to give the desired cyclic hexapeptides, which were purified by reversed-phase HPLC. The linear peptide control compounds were synthesized by standard methods.

Chimeric Peptides

While the synthesis of the L-form of β-turn mimic **5** has been described by Nagai and Sato previously,[47] we found the route cumbersome and difficult to reproduce.[48] An alternative synthesis from L-cysteine and a differently protected form of the δ-aldehyde from glutamic acid was devised on the basis of a synthesis of γ-lactams reported by Baldwin and Lee[49] (Figure 4). The oxazolidinone L-**9** is formed from *N*-carbobenzoxyglutamic acid as described previously.[50] The aldehyde L-**10** is generated in 76% yield from the acid chloride[50] by reduction with n-Bu_3SnH.[51] Condensation of the aldehyde with L-cysteine methyl ester in pyridine over a 5-day period gives the bicyclic, hydroxymethyl derivative L-**11** in 70% yield. The hydroxymethyl group is removed under mildly alkaline conditions to provide the Cbz-protected methyl ester L-**12** in 66% yield after purification by chromatography. The methyl ester is removed with NaOH in methanol and the Cbz protecting group with HBr in acetic acid, and the amine is reprotected as the fluorenylmethoxycarbonyl (Fmoc) derivative L-**14** for use in subsequent peptide coupling reactions. The enantiomeric analog D-**14** is produced from the D-amino acids.

The stereochemistry of the bicyclic turn dipeptide has been assigned on the basis of NOE experiments with the phthaloyl analog,[47] and it was confirmed by NOESY spectroscopy on a sample of the methyl ester L-**12**.

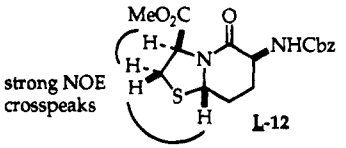

L-12

The tetrapeptides Fmoc-Ala-Trp-Arg(Mtr)-Tyr(*t*-Bu)-OMe and Fmoc-Ser-Trp-Arg(Mtr)-Tyr(*t*-Bu)-OMe were synthesized via standard, solution-phase procedures involving EDC/HOBT coupling of the appropriately protected residues. Removal of the Fmoc moiety and coupling of the tetrapeptides to the bicyclic analogs L-**14** and D-**14** were accomplished in ca. 50% yield under the same conditions. Removal of the Fmoc and methyl ester protecting groups and cyclization with DPPA and $NaHCO_3$ in DMF[40,52] afforded the corresponding cyclic products in 24−43% yields. Side chain protection was removed with TFA in the presence of cation scavengers to give the chimeric peptides L-**7**, D-**7**, and L-**8** in 37−64% overall yields after HPLC purification.

Linear Tri- and Hexapeptides

In part to evaluate the binding affinity of the linear triad of amino acids around which the conformationally constrained

(38) Fletcher, G. A.; Low, M.; Young, G. T. *J. Chem. Soc., Perkin Trans. 1* **1973**, 1162−1164.
(39) Konig, W.; Geiger, R. *Chem. Ber.* **1970**, *103*, 788−98.
(40) Shiori, T.; Ninomiya, K.; Yamada, S. *J. Am. Chem. Soc.* **1972**, *94*, 6203−6205.
(41) Saha, A. K.; Schultz, P.; Rapoport, H. *J. Am. Chem. Soc.* **1989**, *111*, 4856−4859.
(42) Colucci, W. J.; Tung, R. D.; Petri, J. A.; Rich, D. H. *J. Org. Chem.* **1990**, *55*, 2895−2903.
(43) Hudson, D. *J. Org. Chem.* **1988**, *53*, 617−624.
(44) Boden, E. P.; Keck, G. E. *J. Org. Chem.* **1985**, *50*, 2394−2395.
(45) Felix, A. M.; Heimer, E. P.; Lambros, T. J.; Tzougraki, C.; Meienhofer, J. *J. Org. Chem.* **1978**, *43*, 4194−4196.
(46) Bodanszky, M.; Ondetti, M. A.; Birkhimer, C. A.; Thomas, P. L. *J. Am. Chem. Soc.* **1964**, *86*, 4452−4459.
(47) Nagai, U.; Sato, K. *Tetrahedron Lett.* **1985**, *26*, 647−650.
(48) Two other, independent routes to L-*BTD* have been reported recently: Bach, A. C., III; Markwalder, J. A.; Ripka, W. C. *Int. J. Pept. Protein Res.* **1991**, *38*, 314−323. Subasinghe, N. L.; Bontems, R. J.; McIntee, E.; Mishra, R. K.; Johnson, R. L. *J. Med. Chem.* **1993**, *36*, 2356−2361.
(49) Baldwin, R. E.; Lee, E. *Tetrahedron* **1986**, *42*, 6551−6554.
(50) Scholtz, J. M.; Bartlett, P. A. *Synthesis* **1989**, 542−544.
(51) Four, P.; Guibe, F. *J. Org. Chem.* **1981**, *46*, 4439−4445.
(52) Brady, S. F.; Freidinger, R. M.; Paleveda, W. J.; Colton, C. D.; Homnick, C. F.; Whitter, W. L.; Curley, P.; Nutt, R. F.; Veber, D. F. *J. Org. Chem.* **1987**, *52*, 764−769.

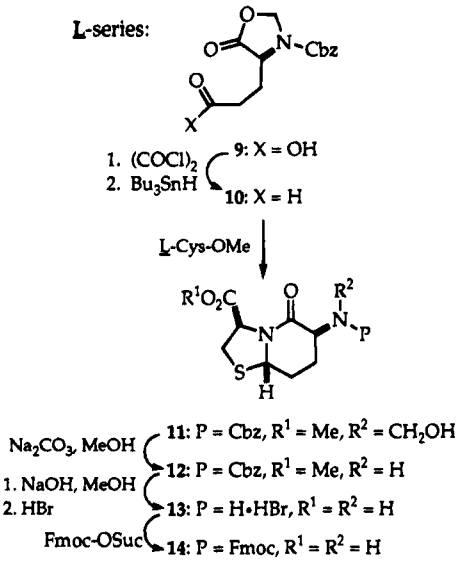

Figure 4. Synthesis of Fmoc-BTD, **14**.

mimics were designed, and in part to explore a limited structure–activity relationship for the residues in this triad, we synthesized and evaluated analogs of Trp-Arg-Tyr itself. This peptide was prepared both in unprotected form (**15**) and as the capped *N*-acetyltripeptide methyl ester **16**, and the Trp and Arg residues were replaced with 2-naphthylalanine (**17**) and with ornithine (**18**) and citrulline (**19**), respectively. To evaluate the importance of conformational constraint on the cyclic hexapeptides **3** and **4**, the corresponding linear analogs Ac-Phe-Ala-Trp-Arg-Tyr-D-Pro-NH_2, **20**, and Ac-Phe-Ser-Trp-Arg-Tyr-D-Pro-NH_2, **21**, were prepared as well using standard solid-phase techniques.

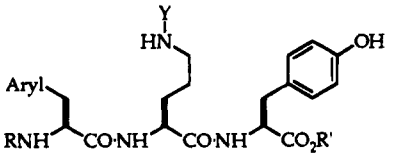

15: Aryl = 3-Indolyl, Y = $C^+(NH_2)_2$, R = H, R' = OH
16: Aryl = 3-Indolyl, Y = $C^+(NH_2)_2$, R = Ac, R' = OMe
17: Aryl = 2-Naphthyl, Y = $C^+(NH_2)_2$, R = Ac, R' = OMe
18: Aryl = 3-Indolyl, Y = H, R = Ac, R' = OMe
19: Aryl = 3-Indolyl, Y = $CONH_2$, R = Ac, R' = OMe
20: Aryl = 3-Indolyl, Y = $C^+(NH_2)_2$, R = Ac-Phe-Ala, R' = D-Pro-NH_2
21: Aryl = 3-Indolyl, Y = $C^+(NH_2)_2$, R = Ac-Phe-Ser, R' = D-Pro-NH_2

Enzyme Assay

A reported assay for α-amylase activity involves the hydrolysis of *p*-nitrophenyl maltoheptoside, with further cleavage of the products with the coupling enzymes α-glucosidase and amyloglucosidase; the eventual signal is produced by release of *p*-nitrophenoxide from smaller oligomers.[53] However, this assay is cumbersome and is not readily applied to the quantitative measurement of K_i values in the micromolar range. We thus developed an assay that involves direct spectrophotometric measurement of a reaction catalyzed by α-amylase, without the use of coupling enzymes. The selectivity of α-amylase toward the various *p*-nitrophenyl maltosides has been studied by Wallenfels et al.[54] Cleavage of these materials is relatively nonspecific and leads to complex product mixtures that complicate the kinetic behavior through further reaction. However,

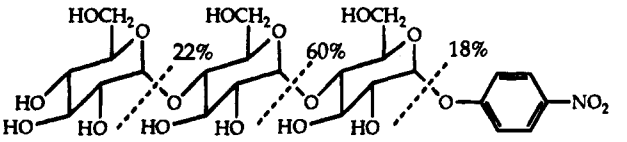

Figure 5. Pattern of cleavage of *p*-nitrophenyl maltotrioside by α-amylase. For release of *p*-nitrophenol; K_m = 1.39 mM and k_{cat} = 1.28 s^{-1} (from Seigner et al.[55]).

Table 1. Inhibition Constants of Tendamistat Mimics[a]

entry	compound	K_i (μM)
	Tripeptides	
1	Ac-Trp-Orn-Tyr-OCH_3 (**18**)	1100[b]
2	Ac-Trp-Cit-Tyr-OCH_3 (**19**)	700[b]
3	Trp-Arg-Tyr (**15**)	520 ± 20[c]
4	Ac-Nap-Arg-Tyr-OCH_3 (**17**)	240 ± 5
5	Ac-Trp-Arg-Tyr-OCH_3 (**16**)	100 ± 3[c]
	Linear Peptides	
6	Ac-Phe-Ala-Trp-Arg-Tyr-D-Pro-NH_2 (**20**)	670 ± 10
7	Ac-Phe-Ser-Trp-Arg-Tyr-D-Pro-NH_2 (**21**)	320 ± 50
	Cyclic Peptides	
8	cyclo[L-BTD-Ser-Trp-Arg-Tyr] (L-**8**)	460 ± 200
9	cyclo[L-BTD-Ala-Trp-Arg-Tyr] (L-**7**)	300 ± 120
10	cyclo[D-BTD-Ala-Trp-Arg-Tyr] (D-**7**)	160 ± 1
11	cyclo[D-Pro-Phe-Ser-Trp-Arg-Tyr] (**4**)	32 ± 2
12	cyclo[D-Pro-Phe-Ala-Trp-Arg-Tyr] (**3**)	14 ± 2

[a] Unless otherwise indicated, assay mixtures contained 40 nM porcine pancreatic amylase I and = 1.8 mM *p*-NPG_3 at pH 6.98; they were incubated at 30 °C and monitored at λ = 405 nm. The values of the kinetic parameters determined for *p*-NPG_3 hydrolysis by α-amylase, k_{cat} = 2.1 ± 0.2 s^{-1} and K_m = 1.8 ± 0.2 mM, are in substantial agreement with those reported previously (k_{cat} = 2.80 s^{-1}, K_m = 1.53 mM).[56] [b] Error limits not determined for these entries because of weak affinity. [c] Competitive inhibition demonstrated.

a convenient assay can be developed on the basis of the hydrolysis of *p*-nitrophenyl maltotrioside (*p*-NPG_3) (Figure 5). This substrate undergoes cleavage at each of the three glycosyl linkages,[55,56] although 18% of the cleavage occurs at the terminal position and releases *p*-nitrophenol. Cleavage at the remaining two linkages destroys substrate, but it does not produce a significant chromophoric change, and the products formed, *p*-NPG_2 and *p*-NPG, are much poorer substrates than *p*-NPG_3 and therefore do not complicate the kinetic analysis by further reaction.

The inhibition constants of the cyclic peptides **3** and **4**, the chimeric BTD-containing peptides D-**7**, L-**7**, and L-**8**, and relevant acyclic control compounds are listed in Table 1. The linear tripeptides Ac-Trp-Arg-Tyr-OCH_3 and Trp-Arg-Tyr were shown to be competitive inhibitors through a full kinetic analysis at three inhibitor concentrations. The K_i values of the mimics and the remaining controls were determined by measuring the reaction rate at five or six different inhibitor concentrations with the substrate concentration fixed at [S] = K_m = 1.8 mM. The acetyltripeptide methyl esters with structurally related side chains (entries 2 and 4) are moderately weaker in binding affinity than the parent, capped tripeptide (entry 5) in spite of the fact that they are more hydrophobic; this observation implies that the polar functional groups on these side chains enter into specific interactions with active site residues. The fact that the parent tripeptides are competitive with substrate further suggests that the inhibitors bind in the active site of α-amylase and is consistent with the view that the conserved triad, Trp-Arg-Tyr, is an important element in the binding interaction of the enzyme with the tendamistat active loop.

(53) Hagele, E.-O.; Schaich, E.; Rauscher, E.; Lehmann, P.; Burk, H.; Wahlefeld, A.-W. *Clin. Chem. (Winston-Salem, N.C.)* **1982**, *28*, 2201–2205.

(54) Wallenfels, K.; Laule, G.; Meltzer, B. *J. Clin. Chem. Clin. Biochem.* **1982**, *20*, 581–586.

(55) Seigner, C.; Prodanov, E.; Marchis-Mouren, G. *Biochim. Biophys. Acta* **1987**, *913*, 200–209.

(56) Ishikawa, K.; Hirata, H. *Arch. Biochem. Biophys.* **1989**, *272*, 356–363.

Comparison between the cyclic (entries 8−12) and the linear hexapeptides (entries 6 and 7) indicates the influence of conformational constraint on the binding affinity of the Trp-Arg-Tyr sequence (the "triad"). The linear hexapeptides are even weaker inhibitors than the capped tripeptide (entry 5) because the additional three amino acids need to be constrained for the triad to fit into the active site. This loss of conformational mobility contributes more of an entropic penalty to the binding equation than is gained from any favorable, additional interactions between these residues and the protein.

The cyclic peptides, however, are significantly better inhibitors than their acyclic counterparts, since less conformational mobility is lost when they fit into the active site. The alanine-containing derivative **3** is bound almost 50-fold more tightly than the acyclic analog (entry 12 vs entry 6), more than overcoming the penalty from adding three residues to the tripeptide. There is less of a penalty in the case of the serine derivative (entry 7), and less gained on cyclization to **4** (entry 11). In comparison to alanine, the serine residue offers the possibility of stabilizing the correct β-turn conformation by a hydrogen bonding interaction with the tyrosine NH group, as well as the liability of a hydrophilic moiety that must be desolvated on binding to the active site. The relative importance of these two effects appears to be different in the case of the acyclic and cyclic hexapeptides. In the former, the serine analog is enhanced as an inhibitor relative to the alanine analog because the conformational influence is paramount; in the latter, where conformation is controlled by cyclization, the relative affinities are reversed. It is interesting to note that Ser is conserved in the corresponding position in four of the five known natural inhibitors of α-amylase. The fifth inhibitor has Asp in this position, which is also known to modify β-turn structures.[57] The X-ray and NMR structures of tendamistat both indicate the existence of a hydrogen bond between the ^{20}Tyr amide NH and the ^{17}Ser hydroxyl oxygen.

The chimeric peptides D-**7**, L-**7**, and L-**8** have even less affinity for α-amylase (entries 8−10), with K_i values comparable to those of the acyclic analogs. Replacement of the D-Pro-Phe unit of **3** and **4** with the BTD moiety, regardless of configuration, has reduced the binding affinity significantly. Since this moiety is less bulky than the dipeptide it replaces, and since our hypothesis concerning the manner in which these inhibitors mimic tendamistat suggests that the linker region of the cyclic peptides does not interact with the enzyme, we infer that the BTD unit is not substituting for the type II′ β-turn and inducing the desired conformation in the Trp-Arg-Tyr triad.

Solution Structures of the Cyclic Peptides and Analogs

To judge the validity of the design process, and to evaluate the observed differences in binding affinities, it was important to determine the solution conformation of the cyclic hexapeptide mimics. The alanine analog **3**, for example, was devised on the basis of the crystal structure of a cyclic hexapeptide of related, but nevertheless different, sequence. Although extensive NMR studies by Kessler et al. have confirmed the similarity of solution- and crystalline-phase conformations in this series,[27] there was no guarantee that the desired conformation would be preserved with markedly different substitution. And, in view of the decrease in binding affinity observed on introduction of the more rigid BTD units in **7** and **8**, it was mandatory to verify whether these moieties were indeed assuming their putative role as β-turn dipeptides.

^{1}H spectra of the mimics were assigned using COSY, ^{1}H^{13}C-COSY,[58] and ROESY techniques.[59] The configuration of the Tyr-Pro amide linkage in the peptides was determined from the ROESY spectra, as well as the chemical shifts of the prolyl β- and γ-carbons.[60] The conformational homogeneity[61,62] of these potentially flexible molecules was established through a combination of $^3J_{HH}$ coupling constants, the temperature dependence of amide proton chemical shifts, and, in the case of **3**, the T_1 relaxation time constants of the carbonyl carbons. Mobility of the peptide backbone was assumed to be independent of side chain flexibility.

Determination of the 3D structures of these medium-sized β-turn mimics by NMR was made possible by the development of ROESY (rotating Overhauser effect spectroscopy) or CAMELSPIN.[59] The volume intensities of ROESY cross-peaks were used to obtain distance constraints for use during energy minimization. The decrease in volume intensity with distance from the carrier was corrected mathematically.[63−66] NOE peaks from flexible side chains were not included in the structure calculations.

Distance−geometry methods[67] are used to generate possible starting conformations that satisfy the distance contraints determined by NMR. Following the lead of Peishoff et al., who found that the conformational space available to cyclic hexapeptides can be explored adequately with 500 starting conformations generated by this approach,[68] we generated a similar number of conformations for the peptides **4** and **7** using a related program, Dspace.[69] In the case of peptide **3**, starting structures were generated using the MultiConformer routine of MacroModel, v3.0.[70]

Assignments

The assignments of all proton spin systems were obtained from DQF-COSY spectra,[71,72] and are given in Table S1 in the supplementary material. Spectra were obtained in DMSO-d_6 to allow assignment of the heteroatom protons without resorting to water suppression techniques, which could affect the integrated intensities. The aromatic side chains were assigned to the corresponding backbone spin system on the basis of strong β-H to aromatic-H NOEs. Both of the cyclic peptide mimics **3** and **4** show medium-strength NOEs between the aromatic rings of Tyr and Phe and the Pro Cα-H protons, confirming the D-stereochemistry of this residue. The ^{13}C T_1 relaxation times of cyclo[D-PFAWRY] (**3**) were determined to evaluate the conformational mobility of different regions of the peptide backbone; the carbon assignments for this compound were determined from the ^{1}H^{13}C-COSY and HMBC (heteronuclear

(57) Abbadi, A.; Mcharfi, M.; Premilat, S.; Boussard, G.; Marraud, M. *J. Am. Chem. Soc.* **1991**, *113*, 2729−2735 and references cited therein.

(58) Bax, A.; Subramanian, S. *J. Magn. Reson.* **1986**, *67*, 565−569.
(59) Bothner-By, A. A.; Stephens, R. L.; Lee, J.; Warren, C. D.; Jeanloz, R. W. *J. Am. Chem. Soc.* **1984**, *106*, 811−813.
(60) Dorman, D. E.; Bovey, F. A. *J. Org. Chem.* **1973**, *38*, 2379−2383.
(61) Kessler, H. *Angew. Chem., Int. Ed. Engl.* **1982**, *21*, 512−523.
(62) Kessler, H.; Griesinger, C.; Lautz, J.; Muller, A.; van Gunsteren, W. F.; Berendsen, H. J. *J. Am. Chem. Soc.* **1988**, *110*, 3393−3396.
(63) Bax, A. *J. Magn. Reson.* **1988**, *77*, 134−147.
(64) Chingas, G. C.; Garroway, A. N.; Bertrand, R. D.; Moniz, W. B. *J. Chem. Phys.* **1981**, *74*, 127−156.
(65) Griesinger, C.; Ernst, R. R. *J. Magn. Reson.* **1987**, *75*, 261−271.
(66) Muller, L.; Ernst, R. R. *Mol. Phys.* **1979**, *38*, 963−992.
(67) Blaney, J.; Crippen, G. Available from QCPE, University of Indiana, Department of Chemistry, Bloomington, IN.
(68) Peishoff, C. E.; Dixon, J. S.; Kopple, K. D. *Biopolymers* **1990**, *30*, 45−56.
(69) Dspace v1.0, Hare Research Inc., Woodinville, WA.
(70) Mohamadi, F.; Richards, N. G. J.; Guida, W. C.; Liskamp, R.; Lipton, M.; Caufield, C.; Chang, G.; Hendrickson, T.; Still, W. C. *J. Comput. Chem.* **1990**, *11*, 440−467.
(71) Wüthrich, K.; Marion, D. *Biochem. Biophys. Res. Commun.* **1983**, *113*, 967−974.
(72) Rance, M.; Sorensen, W. W.; Bodenhausen, G.; Wagner, G.; Ernst, R. R.; Wüthrich, K. *Biochem. Biophys. Res. Commun.* **1983**, *117*, 479−485.

Table 2. Comparison of NH Chemical Shifts (ppm) and $^3J_{\alpha N}$ Coupling Constants (Hz) for Cyclic Peptides in DMSO-d_6 vs 4:1 H_2O/DMSO-d_6 (in Parentheses) at 21 °C, and $^3J_{\alpha N}$ Coupling Constants for BTD-Containing Peptides in DMSO-d_6

	cyclo[D-PFAWRY], **3**		cyclo[D-PFSWRY], **4**		cyclo[BTD-AWRY]	
residue	δ	$^3J_{\alpha N}$	δ	$^3J_{\alpha N}$	L-**7** $^3J_{\alpha N}$	D-**7** $^3J_{\alpha N}$
Phe/BTD	8.76 (8.44)	8.8 (8.4)	8.77 (8.57)	8.8 (8.3)	7.6	6.4
Ala/Ser	7.98 (8.10)	9.0 (7.9)	7.95 (8.12)	9.0 (8.9)	8.1	7.6
Trp	8.17 (7.84)	4.2 (5.0)	8.20 (8.08)	4.4 (3.3)	6.4	9.5
Arg	8.21 (7.77)	7.6 (6.9)	7.79 (7.49)	8.7 (7.5)	3.8	2.5
Tyr	7.31 (7.45)	7.1 (7.7)	7.09 (7.12)	5.7 (7.2)	9.1	8.4

Table 3. ^{13}C Chemical Shifts Used in Assignment of Xaa-Pro Amide Configuration

compound	δ(Cγ) (ppm)	δ(Cβ) (ppm)
cis, general[a]	23.4 ± 0.3	32.2 ± 0.5
trans, general[a]	25.1 ± 0.5	30.5 ± 0.5
cyclo[D-PFAWRY], **3**	24.6	28.2
cyclo[D-PFSWRY], **4**	24.2	28.5
cyclo[D-PFTK(Z)W][b]	24.8	28.2

[a] From Dorman and Bovey.[60] [b] From Kessler et al.[27]

multiple bond correlation)[73,74] spectra (Table S2a). In the case of the serine analog **4**, $^1H^{13}C$-COSY alone was used to determine the assignments for all protonated carbons (Table S2b).

Since conformational differences have been observed for some dipeptide models between DMSO and water,[75] the ^1H spectra of **3** and **4** were also obtained in 4:1 H_2O/DMSO-d_6 to verify that the $^3J_{\alpha N}$ values were not substantially different from those in pure DMSO (the residual 20% DMSO-d_6 was required for solubility). The NH chemical shifts and αH−NH coupling constants for these compounds in the two solvents are compared in Table 2. The COSY spectrum of **4** was also obtained in 4:1 H_2O/DMSO-d_6 to confirm the chemical shift assignments. These spectra are also provided in the supplementary material.

Trans Configuration of Tyr-Pro Amide

Proline residues in cyclic hexapeptides occasionally adopt the *cis* conformation.[29] However, in the cyclic peptides **3** and **4**, no NOE interaction is observed between Pro Cα-H and Tyr Cα-H, which would be expected for the *cis* configuration. In contrast, both mimics exhibit NOEs between the Cδ-H_2 of Pro and the Cα-H of Tyr, consistent with a *trans* Xaa-Pro configuration.[76,77] The chemical shifts of the β- and especially the γ-carbons of the Pro ring have been shown to be sensitive to the configuration of the Xaa-Pro amide bond.[60] The Cβ and Cγ chemical shifts of a series of model peptides, the cyclic peptides **3** and **4**, and the somatostatin analog **1** are given in Table 3. The Tyr-Pro amide bonds in both **3** and **4** were assigned the *trans* configuration on the basis of the 24.6 and 24.2 ppm chemical shifts of the γ-carbons of Pro, respectively. These values of δ(Cγ) are similar to those reported by Kessler et al. for a somatostatin analog to which the *trans* configuration has also been assigned.[27] While the value of δ(Cγ) of **3** lies within the range of chemical shifts associated with the *trans* configuration according to Dorman and Bovey, the value for the Ser derivative **4** lies outside of both the *trans* and *cis* ranges. Moreover, the values of δ(Cβ) for both compounds lie below the assigned range for *trans* isomers.[60] The observed deviations may be due to the rigidity imposed by the cyclic structures, or conceivably to ring-current effects of the nearby Phe or Tyr side chains.

Table 4. Temperature Dependence of Chemical Shifts, $\Delta\delta/\Delta T$ (ppb/K), for NH Hydrogens

residue	**3**	**4**	L-**7**	D-**7**
Phe/BTD	7.32	6.01	3.09	0
Ala/Ser	2.73	2.24	1.60	6.27
Trp	5.36	3.76	2.71	1.85
Arg	4.60	3.45	6.50	5.05
Tyr	0.50	0.90	6.40	8.24

Conformation of Amide Bonds

The temperature dependence of amide proton chemical shifts ($\Delta\delta/\Delta T$) provides a measure of the solvent exposure of these hydrogens (Table 4).[61] A value of $-\Delta\delta/\Delta T < 3.0$ ppb/K indicates that the proton is shielded from the solvent and may be involved in an intramolecular hydrogen bond, while values >6.0 ppb/K suggest that the hydrogen is exposed to solvent.[61] For this reason, as well as the fact that the carbonyl hydrogen bond acceptors cannot be identified, explicit hydrogen bonds were not included as constraints in solving the structures. However, the temperature dependence values were used to modify the partial charges assigned to the nitrogen atoms during the calculations, to compensate for solvent exposure according to the method of Kessler et al.[27]

Dihedral Angles

Dihedral angles were calculated from the Cα-H to NH coupling constants (Table 2) according to the Karplus relationship, using eq 1.[78] After minimization, structures of **3** were

$$^3J_{\alpha N}\,(\mathrm{Hz}) = 6.4\cos^2\theta - 1.4\cos\theta + 1.9 \qquad (1)$$

discarded if any of the five torsions in the backbone were more than 35° from the measured value. For **4** and L-**7**, the allowed ranges of the Φ angles (N−C−C−N) were calculated from the experimentally determined θ angles (H−N−Cα−H)[79] and constrained with a force constant of 1000 kJ/(mol Å)^2 during minimization. The following Φ angle constraints were selected: **4**, Phe, Ser, Arg (−80 > Φ > −160°), Trp (50 > Φ > −50°); L-**7**, Tyr (−80 > Φ > −160°), Arg (50 > Φ > −50°), Ala and L-BTD (−70 > Φ > −170°). The other allowed Φ angle for **4**-Trp and L-**7**-Arg (±120°) was ruled out on the basis of strong CαH to NH NOE cross-peaks.

Distances

Internuclear distances were calculated by calibration of the volume of each cross-peak to that of WN1′-H−4′-H, for which the distance of 2.82 Å is fixed.[80] The dependence of the integrated volume on the offset frequency from the carrier signal was corrected according to eq 2,[27,64,66] in which β_i = arctan-

$$r_{ij} = [(\sin^2\beta_i \sin^2\beta_j)V_{ij}]^{1/6} \qquad (2)$$

($\gamma B_1/\Omega_i$), r_{ij} is the distance between protons i and j, V_{ij} is the integrated volume of the cross-peak, γB_1 is the strength of the applied field in the rotating frame, and Ω_i is the offset of the resonance i from the carrier frequency in hertz.

(73) Bax, A.; Sparks, S. W.; Torchia, D. *J. Am. Chem. Soc.* **1988**, *110*, 7926−7927.
(74) Bax, A.; Summers, M. F. *J. Am. Chem. Soc.* **1986**, *108*, 2093−2094.
(75) Madison, V.; Kopple, K. D. *J. Am. Chem. Soc.* **1980**, *102*, 4855−4863.
(76) Wüthrich, K. *NMR of Proteins and Nucleic Acids*, John Wiley & Sons: New York, 1986; p 290.
(77) Kessler, H.; Anders, U.; Schudok, M. *J. Am. Chem. Soc.* **1990**, *112*, 5908−5916.
(78) Pardi, A.; Billeter, M.; Wüthrich, K. *J. Mol. Biol.* **1984**, *180*, 741−751.
(79) Kline, A. D.; Braun, W. *J. Mol. Biol.* **1988**, *204*, 675−724.
(80) Bye, E.; Mostad, A.; Romming, C. *Acta Chem. Scand.* **1973**, *27*, 471−484.

Table 5. Coupling Constants, $^3J_{\alpha\beta}$ (Hz), and NOE Distance Constraints, d (Å),[a] for Assignment of Prichiral β-hydrogens of Phe and Tyr in **3** and **4**

	cyclo[D-PFAWRY], **3**		cyclo[D-PFSWRY], **4**[b]	
Phe	Phe	Tyr	Phe	Tyr
χ_1	±60°	+60°	±60°	+60°
conformer	g^2t^3/t^2g^3	g^2t^3	g^2t^3/t^2g^3	g^2t^3
$^3J_{\alpha\beta}$	11.8, 3.2	4.3, 9.1	10.6 (β^2), <4.9 (β^3)	<5.3 (β^2), 8.9 (β^3)
$d(\alpha\beta)$	3.0, 2.2	2.4, 2.6	3.0 (β^2), 2.4 (β^3)	2.4 (β^2), –[c] (β^3)

[a] Distances measured from integrated ROESY cross-peaks. [b] Coupling constants measured from the DQF-COSY spectrum. [c] Not observed.

The interresidue cross-peaks used in the structure determination of **3** are given in Table S4 in the supplementary material. Both intra- and interresidue cross-peaks were used in the structure determinations of **4** and L-**7**, with an allowed range of ±0.5 Å from the calculated distances. Cross-peaks involving flexible side chains, as well as those that provided known information, such as NOEs between geminal hydrogens or within aromatic systems, were not used in the calculations.

Side Chain Conformations

In both of the cyclic peptides **3** and **4**, the Cα-H–Cβ-H coupling constants for Tyr and Phe are distinctly different for the two Cβ-H_2 hydrogens, indicating that these side chains adopt single, predominant conformations and allowing stereospecific assignments of the β-hydrogens. The Tyr side chains in both analogs were assigned the g^2t^3 conformation on the basis of their $^3J_{\alpha\beta}$ coupling constants, the α-H–β-H NOEs,[81,82] and the NOEs between the 2′,6′-Tyr aromatic hydrogens and the α- and δ-hydrogens of the Pro ring (Tables 5 and S1). The Cα-H–Cβ-H coupling constants for the Phe side chains of both **3** and **4** indicate that neither occupies the g^2g^3 conformation, although both the t^2g^3 and g^2t^3 conformations are possible. In all three analogs **3**, **4**, and L-**7**, the Trp Cβ-H_2 hydrogens are nearly equivalent in chemical shift and the Cα-H–Cβ-H coupling constants are 7.5 Hz, suggesting that this side chain is mobile. The complexity and overlap of the Arg and Pro methylene multiplets are too severe to assign the prochiral hydrogens of these side chains. The χ_1 angles of the Tyr and Phe residues are consistent with those measured by Kessler et al. for cyclo-[D-PFTK(Z)WF],[27] for which the Phe residue preceding D-Pro occupies a position analogous to that of the Tyr residues in the mimics **3** and **4**. According to the χ_1 angles, both the Phe and Tyr aromatic side chains of **4** are situated over the Pro ring; this conformation of Tyr may not be optimal for a tendamistat mimic, in which the Arg side chain should be sandwiched between the aromatic rings of Tyr and Trp.[83]

Minimization

Starting structures for the minimizations were obtained using the MultiConformer routine[84] in MacroModel[70] (for compound **3**) or through distance randomization using the program Dspace.[69] The structures created in Dspace were initially minimized with constraints using the distance geometry algorithm; they were then reformatted and minimized using the AMBER force field[85] in MacroModel, which allowed us to compare and reject redundant structures automatically.

Cyclo[D-Pro-Phe-Ala-Trp-Arg-Tyr], 3

Figure 6 displays the five lowest energy structures from one of three closely related families from the structure determination of the cyclic peptide **3**. The Trp-Arg-Tyr residues show little variation in conformation between these families, with a β-turn conformation between the Trp and Arg residues that is intermediate between the canonical types I and II′, in that the carbonyl group points away from the side chains. While idealized β-turns have $\Phi_2 = \pm 60°$ and $\Phi_3 = \pm 80-90°$, they are difficult to assign directly by NMR since only the Φ angle is determined by the NH–Cα-H coupling constant, and positive or negative values may or may not be distinguished by NOEs.[76] NOE data and energy minimization may be combined to distinguish between the "carbonyl-down" (types I and II′) and "carbonyl-up" (types I′ and II) conformations, but few β-turns are ideal.[86]

The NMR constraints were also tested for their fit to the backbone conformation of the somatostatin analog **1** that was used as the template for the tendamistat mimics. Experimental distances and angles from the crystal structure of **1** were compared with the data from **3**. The rmsv (root-mean-square violation) was computed to be 50° for the angles and 0.53 Å for the distances. These values are less than the angle and distance rmsv values among the better structures calculated for **3** itself (family A).

Conformational Mobility

One particular relationship is highlighted by the violation calculations. In the various calculated structures, the distance RNα-H–W Cα-H was often found to be >0.5 Å longer and RNα-H–Y NH >1 Å shorter than the values indicated by the NMR data. Since these distances involve the same Arg NH hydrogen, the inconsistency suggests that there is conformational flexibility in this region of the molecule, and that the measured NOE effect reflects averaging on the NMR time scale. To explore this possibility, we determined the ^{13}C T_1 relaxation times for the carbonyl carbons in **3**, which provide an indication of molecular mobility in different regions of the molecule.[87] The T_1 values for **3** measured using the saturation-recovery method are given in Table 6. The relaxation times for the six carbonyl carbons range from 0.7 to 1.7 s, similar to the T_1 values for carbonyls reported for the somatostatin analog **1**.[27] No cross-peaks were observed in the HMBC spectrum for the carbonyls at δ 172.6 (T_1 = 1.25 s) and δ 169.0 ppm (T_1 = 1.69 s), so they cannot be assigned directly; however, it can be inferred by the process of elimination that these resonances belong to the Trp and Tyr carbonyls. The carbonyl carbon at δ 169.0 ppm has a significantly longer T_1 value than the others, suggesting that there is increased mobility in this region. The longer T_1 may belong to the Trp carbonyl, which is not expected to be hydrogen bonded, on the basis of the relatively high $\Delta\delta/\Delta T$ of the Arg NH (4.6 ppb/K) and the model obtained from calculation. Although this assignment is not firm, it is consistent with the proposed flexibility of the Trp-Arg amide suggested above.

Cyclo[D-Pro-Phe-Ser-Trp-Arg-Tyr], 4, and Cyclo[L-BTD-Ala-Trp-Arg-Tyr], L-7

The distances measured from the NOE effects for compounds **4** and L-**7** are also listed in Table S4, and the data used for the

(81) Basus, V. J. In *Methods in Enzymology*; Oppenheimer, N. J., James, T. L., Eds.; Academic Press Inc.: San Diego, CA, 1989; Vol. 176, Part A, pp 132–149.
(82) IUB-IUPAC Commission on Biochemical Nomenclature. *J. Mol. Biol.* **1970**, *52*, 1–9.
(83) Kline, A. D.; Wüthrich, K. *J. Mol. Biol.* **1986**, *192*, 869–890.
(84) Lipton, M.; Still, W. C. *J. Comput. Chem.* **1988**, *9*, 343.
(85) Weiner, S. J.; Kollman, P. A.; Nguyen, D. T.; Case, D. A. *J. Comput. Chem.* **1986**, *7*, 230–252.
(86) Richardson, J. S. *Adv. Protein Chem.* **1981**, *34*, 167–339.
(87) Huntress, W. T., Jr. *J. Chem. Phys.* **1968**, *48*, 3524–3534.

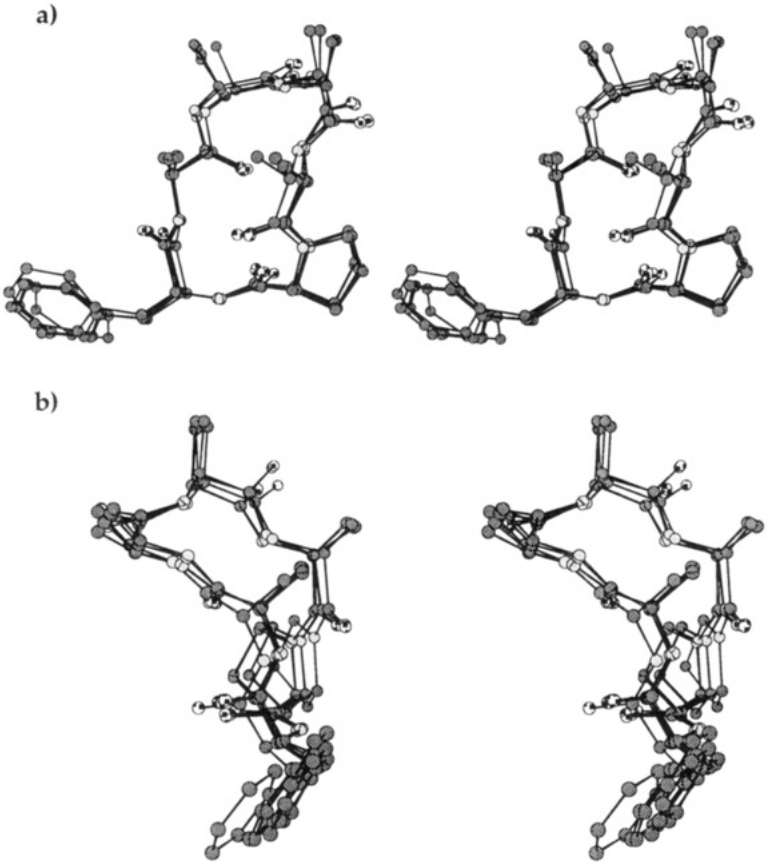

Figure 6. Two views of the favored cluster of backbone conformations determined for cyclo[D-PFAWRY]. Rms violations (rmsv) were calculated for the fit to the NMR data of distances and torsion angles of the backbones in the calculated conformations; structures with average distance rmsv < 0.60 Å and average dihedral rmsv < 14° from the values determined by NMR were grouped into three families on the basis of backbone structural similarity; only family A with the lowest energies and rmsv is shown. Families A and B differ primarily in the conformation of the Pro ring, while family C has a strongly puckered macrocylic ring.

Table 6. Carbonyl ^{13}C T_1 Relaxation Times (s)[a]

cyclo[D-PFAWRY], **3**	Phe	Ala	Trp	Arg	Tyr	-D-Pro
	0.85	0.70	(1.69)	0.93	(1.25)	1.40
cyclo[D-PFTK(Z)WF][b]	Phe	Thr	Lys(Z)	Trp	Phe	-D-Pro
	1.25	1.19	1.16			1.03

[a] T_1 values of carbons for which assignments are not known are indicated in parentheses. [b] From Kessler et al.[27]

assignment of the Phe and Tyr β-hydrogens in **4** are given in Table 5. Random starting conformations were created using Dspace.[69] Each conformation was fully minimized using BatchMin[70] and retained if the energy of the conformer was within 100 kJ/mol of the lowest energy structure. Duplicates were discarded after comparison with all prior structures.

The measured angles, distances, and $\Delta\delta/\Delta T$ values for Ser analog **4** are quite similar to those of the Ala derivative **3** (Tables 2, 5, and S3), and the calculated solution structures are fully consistent. Two key NOEs between hydrogens three residues apart in **4** indicate the dual β-turn conformation anticipated for this cyclic peptide as well. The Tyr NH to Ser NH cross-peak provides strong evidence that the hydrogen bonds Tyr NH···O=C Ser and Ser NH···O=C Tyr are formed in this compound, in analogy to the corresponding interactions in the Ala derivative **3**. An alternative hydrogen-bonding partner for Tyr NH is the Ser hydroxyl oxygen, as found in the structure of tendamistat and proposed in the design of this mimic. Either of these hydrogen-bonding schemes is supported by the low temperature coefficients (Table 4) of the Ser and Tyr NH hydrogens. The differences between the $\Delta\delta/\Delta T$ values for Trp Nα-H and Arg Nα-H between the Ser and Ala mimics may indicate minor differences in the conformations of **3** and **4**.

Several backbone to side chain NOEs were used in the structural determination of **4** (Table S4). In the case of the Ser residue, a number of important NOEs established proximity across the ring. Since the Ser β-hydrogens could not be assigned stereospecifically, the distances were constrained to the carbon atom, and upper limits were increased by the length of a C−H bond, 1.1 Å. The stereoassignments of the Tyr and Phe β-hydrogens (Table 5) permitted the χ_1 angles to be constrained to $\pm 60°$. The NOEs observed between the Pro Cα-H and the Phe and Tyr aromatic hydrogens were included in the form of distance constraints between Pro Cα-H and Phe C4′ and Tyr C4′, respectively, with the upper limit increased by 3.36 Å (the distance between an ortho hydrogen and the para carbon).

The NMR-assignable part of the structure corresponded to cyclo[D-Pro-Phe-Ser-Ala-Ala-Tyr], after removal of the side chains for which no constraints were available. Five hundred starting conformations of this structure were generated by Dspace and then minimized with the AMBER force field to give 63 unique structures that were consistent with the NMR data. The structures were matched by a least-squares superposition (rms) of their backbone atoms and were grouped into six families using the program COMPARE.[67] Two of these families each contained three high-energy structures distorted by γ-turns and were excluded from consideration, since they are rarely found.[86] The AMBER force field appears to overemphasize γ-turns, despite the lowering of partial charges; this effect may be due to the approximation of electrostatic interactions as point charges without directionality. A similar overestimation of γ-turns in molecular dynamics calculations *in vacuo* has also been noted.[27] The remaining four families all include the dual β-turn conformation; the best, A, on the basis of rmsv values for the angles and distances, is represented by the five lowest

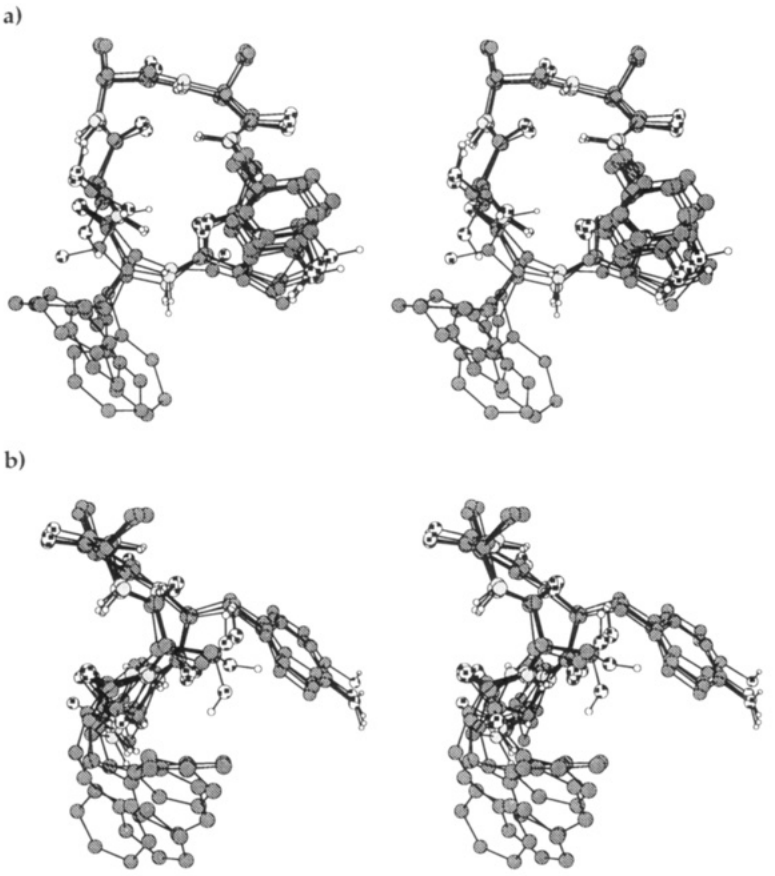

Figure 7. Two views of the favored cluster of backbone conformations determined for cyclo[D-PFSWRY]. The five lowest energy structures of family A are shown.

energy conformers in Figure 7. All of the structures have nonclassical β-turns, although in the various families, both β-turns resemble the canonical type II′ turn better than they do the type I turn.

In all the structures with the lowest angle violations, the two aromatic side chains are in favored, staggered conformations. A slightly puckered macrocyclic ring (Figure 7b) fits the data the best, although the very puckered and very flat extremes cannot be excluded. We also cannot exclude the possibility that the structures found represent a range of conformations in solution.

From the outset, neither of the BTD-templated structures L-**7** and D-**7** appeared to adopt the designed, β-turn conformation, on the basis of the patterns of Cα-H to NH coupling constants and the solvent exposure patterns of the amide hydrogens as determined by the $\Delta\delta/\Delta T$ values (Tables 2 and 4). Both sets of data are significantly different from those found for **3**. Especially notable are the low Cα-H to NH coupling constants of ca. 3−4 Hz for Arg in L-**7** and D-**7**, which resemble the $J_{\alpha N}$ value of the Trp residue in **3** and **4** or the Lys residue in the somatostatin analog **1** (3.4 Hz, Table 2), both of which occupy the $i + 1$ position of a type I β-turn. Similarly, the solvent exposure patterns of L-**7** and L-**8** cannot be accommodated by a structure in which the three residues Trp-Arg-Tyr occupy the same positions as in tendamistat (Table 4). Moreover, there are two long-range ROESY cross-peaks that provide an important indication of the overall conformation of the macrocycle in L-**7**, as shown in Figure 8. NOEs between L-BTD NH and Arg Cα-H (2.99 Å) and between Trp Nα-H and the ring-juncture hydrogen (5-H) of the L-BTD unit (3.12 Å) cannot be accommodated by a conformation with the designed β-turns.

Constrained minimization of 500 starting conformers of L-**7** gave 75 different structures. The structures found are similar to the classic dual β-turn structure of cyclic peptides, except that the turns are located between Arg and Tyr and between the L-BTD unit and Ala, i.e., shifted by one residue in comparison to **3** or **4**. These structures were grouped into four families by COMPARE and represent a range of puckering in the macrocycle, as observed for the cyclic peptide structures described above. Two families (not shown) incorporate an unfavorable half-boat conformation in the six-membered ring of the L-BTD unit, and a γ-turn between the NH of Trp and the C=O of L-BTD. Families C and D have lower overall violations of the distance data, and family D, with the lowest average violation of the dihedral angle data, is represented by the five lowest energy conformers shown in Figure 8.

The one anomalous datum in this assignment is the low $\Delta\delta/\Delta T$ value for Ala NH in analog L-**7** (Table 4); a bifurcated hydrogen bond formed by the L-BTD carbonyl with both Ala NH and Trp NH would fit this datum, and in the best of the calculated structures (Figure 8), these hydrogens are located inside the macrocycle.

The bicyclic moiety L-BTD was originally designed by Nagai and Sato and shown to mimic the type II′ β-turn in gramicidin S, replacing D-Phe at the $i + 1$ position and Pro at the $i + 2$ position.[47] However, in a comprehensive study, involving 29 proteins, of the frequency of occurrence of each amino acid at the four positions of a β-turn, Chou and Fasman found that Pro is 6 times as likely to be found at the $i + 1$ position than at the $i + 2$ position.[88] The inability of the L-BTD unit to mimic a type II′ β-turn in L-**7** may originate in the resemblance of the five-membered ring to Pro, which drives it into the $i + 1$ position. Although the BTD template is a useful mimic of a type II′ β-turn in some circumstances, it does not appear to play this role in substituted cyclic hexapeptides.

(88) Chou, P. Y.; Fasman, G. D. *J. Mol. Biol.* **1977**, *115*, 135−175.

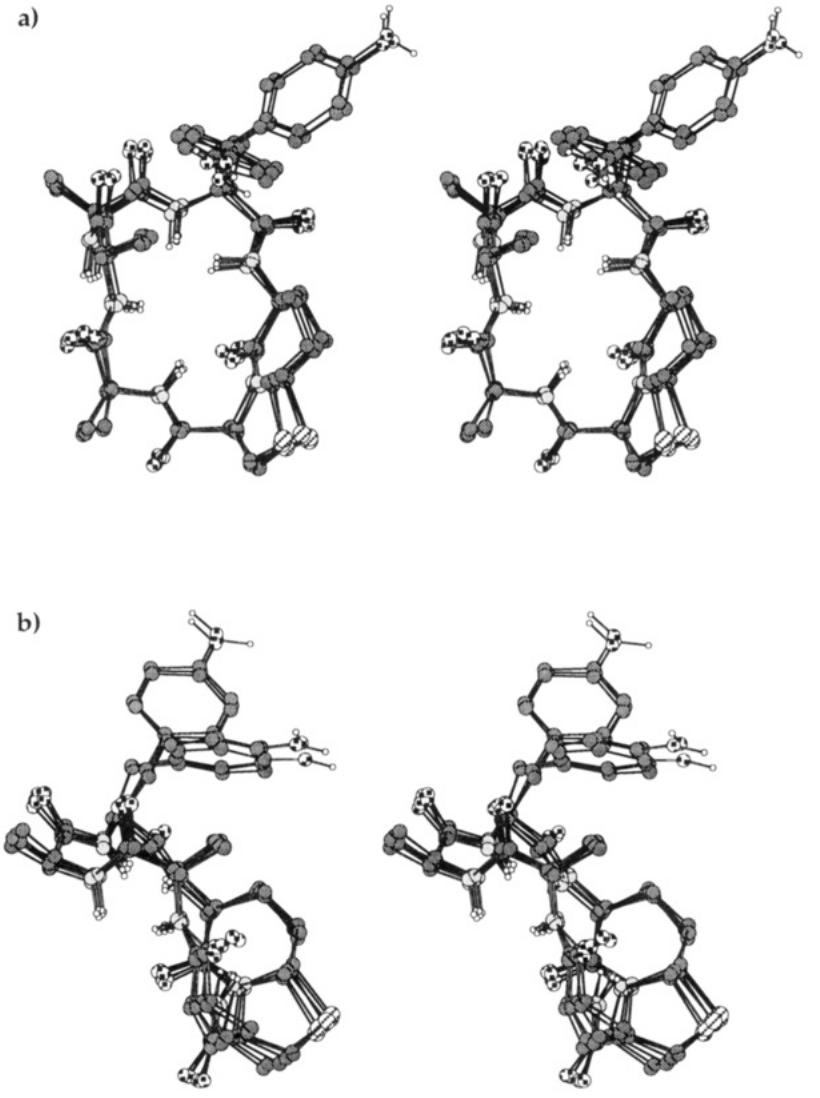

Figure 8. Two views of the favored cluster of backbone conformations determined for cyclo[L-BTD-AWRY]. The six lowest energy structures of family D are shown.

Conclusion

The conformations determined by NMR methods for the two cyclic hexapeptides and the chimeric analog provide a structural rationale for the differences observed in their binding affinities. The β-turn of tendamistat in the vicinity of the Trp-Arg-Tyr residues is reproduced in the cyclic hexapeptides, and these compounds are the most potent of the analogs tested. In contrast, the low-energy conformation of the more weakly bound chimeric derivative L-**7** takes the key residues out of register with the β-turn; this derivative must therefore adopt a higher energy conformation in order to bind to α-amylase in an analogous fashion. These results substantiate the premise on which the tendamistat mimics were designed, in that the combination of the key residues Trp, Arg, and Tyr and an appropriate template is able to imitate the natural inhibitor qualitatively, if not quantitatively. Nevertheless, for none of the derivatives is the conformational issue one of striking quantitative significance; the differences in binding affinities among the most tightly bound, constrained analog (**3**, $K_i = 14$ μM), the weakly bound, incorrectly constrained molecule (L-**7**, $K_i = 300$ μM), and the least tightly bound, unconstrained derivative (**20**, $K_1 = 670$ μM) correspond to less than 2.5 kcal/mole. Since the Trp-Arg-Tyr residues constitute only a fraction of the structure of tendamistat that interacts with α-amylase,[15] it is not surprising that the natural product is bound considerably more tightly ($K_i = 0.2$ nM[10]). However, the fact that a significant portion of this binding affinity can be captured by a small molecule mimic offers considerable encouragement to this structure-based approach to the design of enzyme inhibitors.

Experimental Section

General Procedures. D-Proline, Boc-Phe-OH, 1-[3-(dimethylamino)propyl]-3-ethylcarbodiimide hydrochloride (EDC), and 3,5-dimethylpyrazole-1-carboxamidine nitrate (DMPC) were obtained from Aldrich. Boc-Tyr-OH and Boc-Orn(Z)-OH were obtained from Chemical Dynamics. Fmoc-amino acids were purchased from Bachem. H-Trp-OCH_3, Boc-Ala-OH, Boc-Ser(Bn)-OH, and porcine pancreatic α-amylase (EC 3.2.1.1, type I-A; PMSF-treated, 2× crystallized suspension in 2.9 M NaCl solution containing 3 mM $CaCl_2$) were obtained from Sigma. The substrate, *p*-nitrophenyl maltotrioside (*p*-NPG_3) was obtained from Boehringer Mannheim. All other reagents were obtained from commercial suppliers and used without further purification unless otherwise noted.

All reactions using water- or air-sensitive reagents were conducted under dry N_2 or Ar, with dry solvents. Solvents were distilled under N_2 as follows: CH_2Cl_2 from CaH_2, THF from K, TFA from P_2O_5, *N*-methylmorpholine from CaH_2. DMF was dried over 3 Å molecular sieves, distilled under vacuum, and stored over 3 Å molecular sieves. Reagent grade $CHCl_3$ was washed three times with water, dried (K_2CO_3), and distilled from P_2O_5 to prepare dry, alcohol-free $CHCl_3$. *N,N*-Dimethyl-4- aminopyridine (DMAP) was treated with activated charcoal in ether, filtered while hot, and recrystallized. DMAP·HCl was prepared by bubbling HCl gas through a solution of DMAP in THF; the salt was collected by filtration and dried *in vacuo*.

Evaporation of solvents was performed using a rotary evaporator under water aspirator vacuum. Chromatography refers to flash chromatography on Silica Gel 60 (E. Merck, Darmstadt) according to the method of Still, Kahn, and Mitra.[89] Analytical thin-layer chromatography (TLC) refers to 0.2 mm Silica Gel 60 F-254 (E. Merck) plates visualized with UV light (254 nm) or *p*-anisaldehyde or phosphomolybdic acid spray reagents. HPLC purification was performed on a 22 mm × 25 cm 10 μm Vydac Peptides and Proteins C_{18} column using a flow rate of 5.0 mL/min with UV detection at 280−300 nm, unless otherwise noted.

For NMR spectroscopy, compounds containing Trp were dissolved in $CDCl_3$ which had been freshly filtered through basic Al_2O_3. ^{1}H-NMR spectra were measured on 400 or 500 MHz FT spectrometers. ^{1}H-NMR data are reported as chemical shift (multiplicity, number of protons, coupling constants (Hz)). ^{13}C-NMR spectra were measured at 50.78 or 100.6 MHz; m refers to minor isomer peaks in the ^{13}C spectra. Chemical shifts are reported in parts per million downfield from internal tetramethylsilane (TMS) unless otherwise noted. Mass spectra were determined using fast-atom bombardment (FAB) from a matrix of *o*-nitrobenzyl alcohol, unless otherwise noted.

Amino acid analyses were performed by the Protein Structure Laboratory at the University of California, Davis, CA. Analyses are normalized to the C-terminal amino acid or to Pro in the cyclic peptides, and are reported as: amino acid (calculated, found). Two analyses were performed for each peptide: (1) standard HCl hydrolysis and (2) Trp-conserving methanesulfonic acid (MES) hydrolysis according to Simpson, Neuberger, and Liu.[90] However, the Trp-conserving method gave rise to an artifact that caused the Arg integration to be ca. 5% high, while Trp was still partially destroyed.

Cyclo[D-Pro-Phe-Ala-Trp-Orn(Cbz)-Tyr(Bn)] (by a modification of the macrolactonization procedure of Keck and Boden[44]). The linear peptide Boc-Phe-Ala-Trp-Orn(Cbz)-Tyr(Bn)-D-Pro-OH was prepared by standard solution-phase coupling methods. A 415 mg sample (0.366 mmol) of this material was deprotected by dissolution and stirring in 10 mL of TFA for 15 min. Evaporation of the solvent and precipitation with ether (100 mL) afforded an orange solid that was collected by filtration and dried *in vacuo* to give 0.615 g (69% yield) of the linear peptide H_2N-Phe-Ala-Trp- Orn(Cbz)-Tyr(Bn)-D-Pro-OH. A solution of this hexapeptide·TFA salt in 8:2 $CHCl_3$/DMF (2.8 mL) was added via syringe pump to a solution of EDC (220 mg, 1.15 mmol), DMAP (203 mg, 1.66 mmol), and DMAP·HCl (183 mg, 1.15 mmol) in refluxing $CHCl_3$ (16 mL). The addition was complete after 20 h, and the mixture was cooled to room temperature, diluted with EtOAc (200 mL), washed twice with 1 N HCl (20 mL), twice with saturated $NaHCO_3$ (20 mL), and saturated NaCl (5 mL), and dried (Na_2SO_4). The solvent was evaporated and the product was chromatographed twice (95:5 CH_2Cl_2/MeOH) to give 58 mg (13% yield) of a white solid: ^{1}H NMR ($CDCl_3$) δ 1.24 (m, 5), 1.40 (m, 2), 1.6−2.0 (m, 6), 2.65 (m, 1), 2.82−3.09 (m, 6), 3.45 (m, 3), 4.00 (m, 1), 4.08 (m, 1), 4.40 (m, 1), 4.45 (m, 1), 4.54 (m, 1), 5.02 (m, 3), 5.07 (m, 2), 6.63 (m, 1), 6.84 (d, 2, J = 8.5), 6.91 (m, 1), 7.0−7.2 (m, 8), 7.05 (d, 2, J = 8.5), 7.27−7.40 (m, 14), 7.61 (d, 1, J = 7.8), 8.77 (br s, 1); ^{13}C NMR ($CDCl_3$) δ 17.33, 24.39, 25.73, 28.04, 28.46, 29.62, 37.05, 37.34, 40.36, 47.03, 49.17, 53.77, 54.7, 55.06, 56.50, 60.75, 66.55, 69.82, 109.58, 111.65, 114.76, 118.31, 119.34, 121.92, 123.37, 127.02, 127.29, 127.47, 127.91, 127.98, 128.44, 128.50, 128.69, 129.06, 130.38, 136.15, 136.50, 136.55, 136.80, 156.75, 157.61, 170.57, 171.08, 171.55, 171.90, 172.07, 173.27; $[\alpha]^{22}_D$ = −12.5° (c = 1.04, CH_2Cl_2); IR (CH_2Cl_2) 3419, 3322, 3069, 2936, 2880, 1679 s, 1631 s, 1512 s, 1456 cm^{-1}; HRMS calcd for $C_{57}H_{63}N_8O_9$ (M^+) m/z = 1003.4718, found m/z = 1003.4717.

Cyclic dimer (22 mg, 6.0% yield) was isolated in addition to the desired cyclic monomer. The ^{1}H NMR spectrum ($CDCl_3$) showed a doubling of all peaks, implying that the macrocycle was not symmetrical by conformational averaging. MS m/z = 2006 (MH^+).

Cyclo[D-Pro-Phe-Ala-Trp-Arg-Tyr]·CF_3CO_2H, 3. A mixture of the protected cyclic peptide (66 mg, 0.066 mmol), 10% Pd/C (66 mg), and 20% $Pd(OH)_2$/C (66 mg) was flushed thoroughly with N_2, and a solution of 1.6 M NH_4HCO_3 in HOAc (0.55 mL, 0.87 mmol) was added. After 3.5 h, the catalysts were removed by filtration through a Millipore filter and rinsed with MeOH, and the solvents were evaporated to give 52 mg (95% yield) of the deprotected peptide as a white powder: ^{1}H NMR (CD_3OD) δ 1.0−1.3 (m, 3), 1.3−1.48 (m, 1), 1.51 (d, 3, J = 7.2), 1.58−1.88 (m, 6), 1.93 (s, 3), 2.62 (m, 2), 2.76−2.86 (m, 3), 2.98 (dd, 1, J = 4.4, 12.8), 3.37 (m, 2 obscured by residual solvent peak), 3.91 (dd, 1, J = 4.4, 9.7), 4.12 (dd, 1, J = 5.6, 7.7), 4.28 (dd, 1, J = 7.6, 7.6), 4.51 (m, 2), 4.64 (dd, 1, J = 4.5, 9.9), 6.68 (d, 2, J = 8.5), 7.01−7.28 (m, 9), 7.35 (d, 1, J = 8.0), 7.57 (d, 1, J = 8.0). Triethylamine (0.047 mL, 0.33 mmol) was added to a solution of the deprotected peptide (33 mg, 0.039 mmol) and DMPC (25 mg, 0.12 mmol) in DMF (0.22 mL) under N_2. The mixture was warmed to 40 °C for 4 h, cooled to room temperature, and stirred for another 24 h. The product was precipitated with H_2O (1.5 mL), collected by filtration, rinsed with H_2O (1 mL), and collected by dissolution in MeOH, and the solvent was evaporated. (Product may also be recovered from the aqueous wash.) The off-white solid was purified by HPLC (0.05% TFA/45:55 H_2O/MeOH) to give 14 mg (41% yield) of the cyclic peptide **3** as a white powder: ^{1}H NMR (CD_3OD) δ 1.1−1.3 (m, 3), 1.45−1.47 (m, 1), 1.50 (d, 3, J = 7.2), 1.60−1.84 (m, 6), 2.76−2.85 (m, 3), 2.94−3.00 (m, 3), 3.37 (m, 2 obscured by residual solvent peak), 3.95 (dd, 1, J = 5.1), 4.12 (dd, 1, J = 5.6, 7.8), 4.30 (dd, 1, J = 7.6, 7.6), 4.50 (dd, 2, J = 4.0, 10.8), 4.63 (dd, 1, J = 4.6, 9.9), 6.68 (d, 2, J = 8.5), 7.01−7.27 (m, 9), 7.34 (d, 1, J = 8.0), 7.57 (d, 1, J = 8.0) (^{1}H and ^{13}C assignments in DMSO-d_6 are given in Tables S1 and S2, respectively, in the supplementary material); $[\alpha]^{22}_D$ = −19.1° (c = 1.38, MeOH); FTIR (KBr) 3320.9 s, 1669.8 s, 1637.4 s, 1534.8, 1516.0, 1453.4, 1202.1, 1135.8 cm^{-1}; amino acid analysis (1) Phe (1.00, 1.00), Ala (1.00, 0.99), Arg (1.00, 0.95), Tyr (1.00, 0.91), Pro (1.00, 1.00), (2) Phe (1.00, 0.94), Ala (1.00, 0.98), Trp (1.00, 0.60), Arg (1.00, 0.93), Tyr (1.00, 0.93), Pro (1.00, 1.00); HRMS (FAB^+, glycerol/thioglycerol matrix) calcd for $C_{43}H_{52}N_{10}O_7$ (MH^+) m/z = 821.4099, found m/z = 821.4101.

Cyclo[D-Pro-Phe-Ser-Trp-Arg-Tyr]·CF_3CO_2H, 4. **4** was prepared as described for the alanine analog **3**. The crude product was purified by HPLC (0.1% TFA/65:35 H_2O/CH_3CN) to give 6 mg (21% yield) of **4** as a white solid: ^{1}H NMR (DMSO-d_6, 500 MHz) δ 1.2−1.45 (m, 4), 1.64 (m, 2), 1.77 (m, 2), 2.60 (dd, 1, J = 12.6, 8.6), 2.65 (m, 1), 2.71 (dd, 1, J = 14.1, 12.0), 2.95 (dd, 1, J = 12.6, 4.8), 3.00 (m, 2), 3.10 (m, 2), 3.25 (dd, 1, J = 14.1, 3.2), 3.31 (m, obscured by H_2O peak), 3.90 (m, 2), 4.03 (dd, 1, J = 7.9, 5.4), 4.08 (ddd, 1, J = 18.0, 9.0, 5.7), 4.16 (m, 1), 4.27 (ddd, 1, J = 11.7, 8.5, 3.2), 4.51 (m, 1), 4.54 (m, 1), 5.53 (br s, 1), 6.66 (d, 2, J = 8.4), 6.91 (d, 2, J = 7.7), 6.98 (t, 1, J = 7.7), 7.06 (t, 1, J = 7.0), 7.10 (d, 1, J = 5.7), 7.16 (m, 1), 7.20−7.25 (m, 5), 7.35 (d, 1, J = 8.1), 7.49 (d, 1, J = 8.0), 7.79 (d, 1, J = 8.5), 8.21 (d, 1, J = 4.2), 8.78 (d, 1, J = 9.1), 9.32 (s, 1), 10.89 (s, 1) (^{1}H and ^{13}C assignments in DMSO-d_6 are given in Tables S1 and S2, respectively, in the supplementary material); amino acid analysis (1) Phe (1.00, 1.01), Ser (1.00, 0.88), Arg (1.00, 0.92), Tyr (1.00, 0.95), Pro (1.00, 1.00), (2) Phe (1.00, 0.98), Ser (1.00, 0.87), Trp (1.00, 0.76), Arg (1.00, 0.99), Tyr (1.00, 0.97), Pro (1.00, 1.00); HRMS calcd for $C_{43}H_{53}N_{10}O_8$ (MH^+) m/z = 837.4048, found m/z = 837.4037.

Fmoc-L-BTD-Ala-Trp-Arg(Mtr)-Tyr(*t*-Bu)-OMe. Fmoc-L-BTD, L-**14**, and Ala-Trp-Arg(Mtr)-Tyr(*t*-Bu)-OMe were coupled according to standard procedures using EDC and HOBT; from the tetrapeptide (395 mg, 0.36 mmol), 235 mg (50%) of the hexapeptide was obtained as a white solid: TLC R_f 0.57 (9:1 $CHCl_3$/MeOH); MS m/z = 1298 (MH^+), 1320 (M + Na); ^{1}H NMR ($CDCl_3$) (only the following characteristic peaks were assigned) δ 9.12 (br s, 1, Trp 1-NH), 7.75 (d, 2, J = 7.7, Fmoc 4,5-H), 6.83 (d, 2, J = 8.4, Tyr 3,5-H), 3.80 (s, 3, Mtr 4-OMe), 3.59 (s, 3, Tyr OMe), 2.71 (s, 3, Mtr 5-Me), 2.64 (s, 3, Mtr 2-Me), 2.12 (s, 3, Mtr 3-Me), 1.27 (s, 9, *t*-Bu).

Cyclo[L-BTD-Ala-Trp-Arg-Tyr], L-7. A solution of the fully protected, linear hexapeptide (200 mg, 0.15 mmol) in CH_2Cl_2 (1 mL) was treated with Et_2NH (0.5 mL, excess) at room temperature for 5 h. The resulting cloudy solution was evaporated to dryness and washed with Et_2O (4 × 3 mL). The solid was dissolved in MeOH (2 mL), and the solution was treated with 1 N NaOH (0.34 mL, 2.2 eq) at 0 °C to room temperature for 8 h. The reaction mixture was acidified with 1 N HCl to pH 1 and evaporated to a white solid. The crude product was dissolved in 1 mL of MeOH and chromatographed on a Sephadex LH-20 column (12 mm × 10 in, eluted with MeOH) to give 183 mg of a white solid: TLC R_f 0.15 (9:1:0.1 $CHCl_3$/MeOH/Et_3N); MS m/z =1062 (MH^+).

(89) Still, W. C.; Kahn, M.; Mitra, A. *J. Org. Chem.* **1978**, *43*, 2923−2925.

(90) Simpson, R. J.; Neuberger, M. R.; Liu, T.-Y. *J. Biol. Chem.* **1976**, *251*, 1936−1940.

A solution of the end-deprotected peptide (183 mg, 0.15 mmol) in anhydrous DMF (20 mL) was cooled to 0 °C under a stream of Ar, and DPPA (65 μL, 2 equiv) was added slowly, followed by solid $NaHCO_3$ (63 mg, 5 equiv). The mixture was stirred vigorously at 0 °C for 3.5 days, at which time TLC (9:1 $CHCl_3$/MeOH) showed very little starting peptide left. H_2O (4 mL) was added while maintaining the temperature at 0 °C. The resulting clear solution was stirred with 2 g of Bio-Rad AG501-X8D mixed bed (indicating) ion exchange resin for 4 h. The resin was separated by filtration and washed with 4 mL of 4:1 DMF/H_2O; the filtrate was evaporated to give a yellow, oily residue. The crude product was chromatographed (silica gel, eluted first with an EtOAc/hexanes gradient and then with 5% MeOH/EtOAc) to give 49 mg (32%) of the cyclic peptide as a white solid: TLC R_f 0.50 (9:1 $CHCl_3$/MeOH); MS m/z = 1043 (MH^+), 1065 (M + Na); ^1H NMR ($CDCl_3$) (only the following characteristic peaks were assigned) δ 3.74 (s, 3, Mtr 4-OMe), 2.64 (s, 3, Mtr 5-Me), 2.55 (s, 3, Mtr 2-Me), 2.04 (s, 3, Mtr 3-Me), 1.19 (s, 9, *t*-Bu).

The protected, cyclic peptide (45 mg, 43 μmol) was stirred with a premixed cocktail consisting of 90% TFA, 5% thioanisole, 3% ethanedithiol, and 2% anisole (5 mL) at room temperature under Ar for 5 h, at which time TLC (7:7:5:1 EtOAc/*i*-PrOH/H_2O/NH_4OH) indicated that no starting material was left. The reaction mixture was diluted with cold Et_2O (30 mL), the resulting suspension was centrifuged, and the supernatant was removed. The pellet was washed with Et_2O (3 × 10 mL) and dried under a stream of Ar to furnish 22 mg (66%) of L-**7** as a white solid. Final purification by HPLC (Vydac C18, 10 μm, 250 mm × 22.5 mm, detection at 275 nm, flow rate 5 mL/min, 50% CH_3CN/H_2O containing 0.1% TFA) provided 20 mg (64%) of the desired cyclic peptide as a white solid: TLC R_f 0.50 (EtOAc/*i*-PrOH/H_2O/NH_4OH); HRMS calcd for $C_{37}H_{47}N_{10}O_7S$ (MH^+) m/z = 775.3350, found m/z = 775.3362. NMR data for this compound are presented in Tables S1 and S2.

Cyclo[D-BTD-Ala-Trp-Arg-Tyr], D-7. D-**7** was prepared as described above for L-**7**. From the cyclic protected peptide (110 mg, 0.11 mmol), 51.4 mg (60%) of the deprotected product was obtained as a white solid after HPLC: TLC R_f 0.44 (EtOAc/*i*-PrOH/H_2O/NH_4OH); HRMS calcd for $C_{37}H_{47}N_{10}O_7S$ (MH^+) m/z = 775.3350, found m/z = 775.3346. NMR data for this compound are presented in Tables S1 and S2.

Cyclo[L-BTD-Ser-Trp-Arg-Tyr], L-8. The acyclic precursor was deprotected according to the proce dure described above for L-**7**. From 85 mg (76 μmol) of the linear material, 22 mg (37%) of the desired cyclic peptide was obtained as a white solid after HPLC purification: TLC R_f 0.20 (EtOAc/*i*-PrOH/H_2O/NH_4OH); HRMS calcd for $C_{37}H_{47}N_{10}O_8S$ (MH^+) m/z = 791.3299, found m/z = 791.3287. NMR data for this compound are presented in Tables S1 and S2.

(*S*)-3-Carbobenzoxy-5-oxo-1,3-oxazolidine-4-propanal, L-10. A solution of the acid L-**9**[50] (10.3 g, 35.2 mmol) in CH_2Cl_2 (100 mL) was treated with $(COCl)_2$ (6.1 mL, 2 equiv) in the presence of a catalytic amount of DMF (0.10 mL, 4 mol %) at room temperature for 14 h. The reaction mixture was evaporated to a colorless oil, and the crude acid chloride was redissolved in anhydrous EtOAc (300 mL). Bu_3SnH (10 g, 1.0 equiv) was added with stirring via a syringe pump at 0 °C under Ar over a 1.5 h period, and the resulting solution was allowed to warm from 0 °C to room temperature for 14 h. The mixture was worked up by washing with H_2O (2 × 200 mL) and saturated NaCl (200 mL), drying over $MgSO_4$, and evaporating under reduced pressure. The oily residue was dissolved in 250 mL of CH_3CN and washed with petroleum ether (5 × 100 mL). Evaporation of the CH_3CN layer gave 9.92 g (100%) of the aldehyde as a yellow oil that was carried on without purification: TLC R_f 0.56 (1:1 EtOAc/hexanes); ^1H NMR ($CDCl_3$, 250 MHz) δ 9.30 (s, 1, CHO), 7.30 (m, 5, C_6H_5-), 5.46 (s, 1, 2-H_a), 5.15 (m, 3, 2-H_b and benzyl CH_2), 4.30 (t, 1, J = 5.5, 4-H), 2.54 (br s, 2, 7-H), 2.20 (m, 2, 6-H).

Cbz-L-BTD-OMe, L-12. L-Cys-OMe·HCl (3.2 g, 0.7 equiv; Sigma) was added in one portion to a stirring solution of the crude aldehyde L-**10** (7.4 g, 27 mmol) in pyridine (250 mL, freshly distilled from CaH_2) at room temperature under Ar, and the resulting clear solution was left to stand at room temperature for 5 d. The solvent was evaporated under reduced pressure to give a yellow oil, which was dissolved in 250 mL of EtOAc. The resulting cloudy solution was washed with saturated NH_4Cl (250 mL), H_2O (250 mL), and saturated NaCl (250 mL), dried over $MgSO_4$, and evaporated to yield a yellow oil. Chromatography (silica gel, EtOAc/hexanes gradient) gave 5.2 g (71%) of pure condensation product, *N*-(hydroxymethyl)-Cbz-L-BTD-OMe, L-**11**, as a white foam: TLC R_f 0.77 (9:1 $CHCl_3$/MeOH); ^1H NMR ($CDCl_3$) δ 7.34 (m, 5, C_6H_5-), 5.60−4.20 (m, 7, benzyl CH_2, 2,5,8-H and OCH_2N), 3.72 (s, 3, OMe), 3.33 (m, 1, 3-H_a), 3.15 (m, 1, 3-H_b), 2.50−2.10 (m, 3, 7-H_a,H_b, 6-H_a), 1.89 (m, 1, 6H_b); ^{13}C NMR ($CDCl_3$) δ 170.0, 167.8, 155.3, 136.1, 128.6, 128.4, 128.0, 68.1, 67.6, 62.6, 61.3, 53.9, 52.7, 31.6, 28.1, 26.5.

A solution of the bicyclic dipeptide L-**11** (0.92 g, 2.3 mmol) in anhydrous MeOH (25 mL) was stirred with solid Na_2CO_3 (20 mg, 0.1 equiv) at room temperature for 4 h. The reaction mixture was evaporated, and the crude product was chromatographed (silica gel, EtOAc/hexanes gradient) to give 0.56 g (66%) of the desired product as a white solid, along with recovery of 0.12 g (13%) of starting material: TLC (product) R_f 0.36 (1:1 EtOAc/hexanes); $[\alpha]_D$ = −170° (c = 0.0010, MeOH); ^1H NMR ($CDCl_3$) δ 7.32 (m, 5, C_6H_5-), 5.63 (s, 1, NH), 5.08 (m, 3, benzyl CH_2, and 2-H), 4.89 (dd, 1, J = 10.6, 4.4), 4.18 (br s, 1, 8-H), 3.72 (s, 3, OMe), 3.31 (dd, 1, J = 11.6, 8.3, 3-H_a), 3.14 (dd, 1, J = 11.6, 5.7, 3-H_b), 2.51 (br s, 1, 7-H_a), 2.30 (m, 1, 6H_a), 1.80 (m, 2, 7-H_b, 6-H_b); ^{13}C NMR ($CDCl_3$) δ 170.3, 167.1, 156.4, 136.2, 128.3, 127.9, 127.8, 66.7, 62.7, 60.5, 52.8, 51.8, 31.7, 27.8, 27.5. NOESY spectroscopy ($CDCl_3$, mixing time 1 s) showed that the bridgehead proton 5-H has an NOE cross-peak with the Pro-S 3-H but no NOE cross-peak with the Pro-R 3-H. MS m/z = 365 (MH^+), 387 (M + Na); HRMS calcd for $C_{17}H_{21}N_2O_5S$ (MH^+) m/z = 365.1168, found m/z = 365.1171.

H-L-BTD-OH, L-13. A solution of the methyl ester L-**12** (154 mg, 0.42 mmol) in MeOH (1 mL) was treated with 1 N NaOH (0.9 mL, 2.2 eq) at 0 °C for 4 h. The reaction mixture was concentrated to 1 mL, diluted with 2 mL of H_2O, adjusted to pH 1 with 1 N HCl, and then extracted with EtOAc (4 × 3 mL). The organic layer was washed with saturated NaCl (5 mL), dried over $MgSO_4$, and evaporated to a white foam: TLC R_f 0.15 (9:1:0.1 $CHCl_3$/MeOH/AcOH); ^1H NMR ($CDCl_3$) δ 8.36 (br s, 1, COOH), 7.32 (m, 5, C_6H_5-), 6.95 (br s, 1, NH), 5.09 (s, 2, benzyl CH_2), 5.05 (d, 1, J = 7.2, 2H), 4.83 (br s, 1, 5-H), 4.23 (br s, 1, 8-H), 3.31 (dd, 1, J = 11.8, 8.4, 3-H_a), 3.19 (m, 1, 3-H_b), 2.41 (br s, 1, 7-H_a), 2.28 (br s, 1, 6H_a), 1.86 (m, 2, 7-H_b, 6-H_b); ^{13}C NMR ($CDCl_3$) δ 172.4, 168.5, 157.0, 136.5, 128.8, 128.4, 128.3, 67.5, 63.4, 61.3, 52.1, 31.9, 28.0, 27.7; HRMS calcd for $C_{16}H_{19}N_2O_5S$ (MH^+) m/z = 351.1016, found m/z = 351.1015.

The crude acid was stirred with 30% HBr/AcOH (1 mL, 10 equiv) at room temperature for 10 min, with vigorous evolution of gases in the first few minutes. The mixture was diluted with Et_2O (5 mL) to precipitate the product, the resulting suspension was centrifuged, and the supernatant was removed. The pellet was washed with Et_2O (3 × 3 mL), dried under a flow of Ar, and evacuated in the presence of NaOH to give 119 mg (95% from the methyl ester L-**12**) of the desired salt as a white solid: TLC R_f 0.0 (9:1:0.1 $CHCl_3$/MeOH/AcOH); ^1H NMR (CD_3OD) δ 8.50 (br s, 1, COOH?), 5.02 (dd, 1, J = 8.1, 6.1, 2-H), 4.93 (dd, 1, J = 10.4, 4.1, 5-H), 4.01 (dd, 1, J = 11.5, 5.7, 8-H), 3.47 (dd, 1, J = 11.7, 8.2, 3-H_a), 3.18 (dd, 1, J = 11.7, 6.0, 3-H_b), 2.44 (m, 2, 7-H_a, 6-H_a), 2.00 (m, 2, 7-H_b, 6-H_b); ^{13}C NMR (CD_3OD, 100 MHz) δ 173.1, 165.6, 64.0, 62.3, 51.0, 32.6, 27.9, 26.5; HRMS calcd for $C_8H_{13}N_2O_3S$ (MH^+) m/z = 217.0651, found m/z = 217.0647.

Fmoc-L-BTD-OH, L-14. A solution of the HBr salt L-**13** (119 mg, 0.40 mmol) in 10% Na_2CO_3 (1 mL, 2.2 equiv) was added slowly to a vigorously stirred solution of *N*-(Fmoc-O)succinimide (212 mg, 1.5 equiv) in DME (2 mL), and the resulting suspension was stirred at room temperature for 3 h. The reaction mixture was diluted with H_2O (10 mL) and extracted with Et_2O (3 mL) and EtOAc (2 × 3 mL). The aqueous phase was cooled in an ice bath and acidified with concentrated HCl to pH 1. The cloudy aqueous solution was extracted with EtOAc (5 × 3 mL), and the organic layer was washed with saturated NaCl (5 mL), dried over $MgSO_4$, and evaporated to give 152 mg (87%) of the Fmoc-protected acid L-**14** as a white foam: TLC R_f 0.20 (9:1:0.1 $CHCl_3$/MeOH/AcOH); ^1H NMR (acetone-d_6, 500 MHz) δ 7.84 (d, 2, J = 7.5, Fmoc 4,5-H), 7.71 (d, 2, J = 7.0, Fmoc 1,8-H), 7.39 (t, 2, J = 6.7, Fmoc 3,6−H), 7.31 (t, 2, J = 6.2, Fmoc 2,7-H), 5.11 (br s, 1, 2-H), 4.96 (br s, 1, 5-H), 4.29 (m, 4, 8-H and Fmoc 9,10-CH_2), 3.45 (dd, 1, J = 11.5, 8.3, 3-H_a), 3.19 (dd, 1, J = 11.3, 5.3, 3-H_b), 2.40 (br s, 1, 6-H_a), 2.28 (br s, 1, 7-H_a), 2.02 (m, 2, 6,7-H_b). ^{13}C NMR (acetone-d_6, 125 MHz) δ 171.4, 168.1, 156.5, 144.0, 142.0, 128.4, 127.9, 126.2,

120.7, 67.2, 63.3, 61.5, 47.9, 32.1; HRMS calcd for $C_{23}H_{23}N_2O_5S$ (MH^+) m/z = 439.1327, found m/z = 439.1328.

Enzyme Assays. The buffer used for all assay solutions was 25 mM HEPES (*N*-(2-hydroxyethyl)piperazine-*N'*-ethane-2-sulfonic acid) containing 50 mM NaCl and 5 mM $CaCl_2$ at pH 6.98 ± 0.02. HEPES has been shown to minimize the effects of temperature on amylase activity assays.[91] Stock solutions of *p*-NPG_3 (51 mM) were prepared in the same buffer. Stock solutions of the enzyme were stabilized with 0.1 mg/mL BSA (bovine serum albumin). The concentrations of inhibitor solutions were determined by UV at 280 nm using ϵ = 6380 M^{-1},[92] except for the naphthylalanine analog **17**, for which $\epsilon(282)$ = 8800 M^{-1} was used. The assays were conducted at 30 °C using a UVIKON 860 UV/vis spectrophotometer; the buffer and inhibitor stock solutions were maintained at 30 °C. For K_m measurements, five quartz cuvettes were charged with a measured amount of buffer, 20 μL of enzyme stock solution containing 2.4 μM α-amylase, and the reaction was initiated by addition of 20 μL to 100 μL of *p*-NPG_3 in buffer for final concentrations of 1.0, 2.0, 3.0, 4.1, and 5.1 mM in a total volume of 1.0 mL. For inhibition studies, 20−500 μL of the inhibitor stock solution was added to the cuvettes prior to addition of 35 μL of *p*-NPG_3 stock solution (final concentration 1.8 mM). The rate of formation of *p*-nitrophenol was monitored at 405 nm for 20 time points over a 10 min period The total absorbance change during the assay ranged from 0.1 to 0.5, representing ≤10% of the reaction. Values for V_{max} and K_i were determined by fitting the data to eq 3 with a nonlinear least-squares algorithm.

$$V = \frac{[S]V_{max}}{[S] + K_m(1 + [I]/K_i)} \quad \text{for } [S] = K_m, \quad V = \frac{V_{max}}{2 + [I]K_i} \tag{3}$$

NMR Experimental Details. General Procedures. Each sample was dissolved in 0.5−0.6 mL of DMSO-d_6 which had been dried over 3 Å molecular sieves for several days. Solutions were degassed by 3−5 freeze−pump−thaw cycles and sealed under vacuum. COSY and ROESY spectra were obtained on a Bruker AM500 spectrometer. ^{13}C spectra and ^{13}C T_1 relaxation measurements were performed on a Bruker AM400 with a Q-probe. The H,C-heteronuclear 2D spectra were obtained on a Bruker AMX400 with a Q-probe using inverse (^1H) detection. Pulse sequences and representative spectra are provided in the supplementary material.

Structure Elucidation of Cyclo[D-Pro-Phe-Ala-Trp-Arg-Tyr], 3. The cross-peak volumes from the ROESY experiment at a mixing time of 200 ms were integrated using Bruker UXNMR. Cyclo[D-Pro-Ala-Ala-Ala-Ala-Ala] was used as the input structure for the MultiConformer run and initial backbone minimizations. The closure bonds were chosen to be the amide bond between ^{1}Ala and ^{2}Ala (0.5−5.0 Å closure window, 140°−220° closure angle) and the Pro Cβ−Cγ bond (1−2 Å closure window). Resolution was 60° for each bond within the macrocyclic ring and the Pro ring, excluding amide bonds (maintained at 180°) or the bonds adjacent to the closure bonds. The nonbonded interaction cutoff was set to 1.5 Å. Interresidue distance constraints based on NOEs were used to discard structures for which interproton distances were >3.5 Å representing two strong NOEs and >4.5 Å for seven other backbone NOEs (Table S4). Two searches were performed, both with 60° resolution. A search of all dihedral angle combinations of 0, 60, 120, 180, −120, and −60° produced 44 conformers, while searching 30, 90, 150, −150, −90, and −30° produced 207 conformers, a total of 251.

Starting conformations were minimized for 1000 iterations using the AMBER force field as implemented in Batchmin v2.6.[70] Distances were constrained to ±0.5 Å of the NMR measured values with a force constant of 20.0 kJ/(mol Å^2) during minimizations. Structures with any torsion angle more than ±35° from the NMR measured values were discarded after minimization. Side chains were added to five different resulting backbone structures. Each of these five complete conformers was again searched using the MultiConformer routine, to give 677 conformations all told. These conformers were minimized with the constraints given in Table S4.

Modeling of Cyclo[D-Pro-Phe-Ser-Trp-Arg-Tyr], 4, and Cyclo-[L-BTD-Ala-Trp-Arg-Tyr], L-7. The cross-peak volumes from the ROESY experiment at a mixing time of 200 ms were integrated using Felix.[93] The volumes were converted into distances using a program written in C (supplementary material) to correct for offset from the carrier. The side chains for which no stereospecific assignments of the β-hydrogens could be obtained were stripped from the input structures to give cyclo[L-BTD-^{1}Ala-^{2}Ala-^{3}Ala-Tyr] and cyclo[D-Pro-Phe-Ser-^{1}Ala-^{2}Ala-Tyr]. The "embed" command in Dspace was used to create 500 randomized starting structures which were then minimized with 320 iterations with constraints. Partial minimization of the randomized structures in Dspace was required before conversion of PDB coordinates to MacroModel format.

The 500 structures were minimized with the AMBER force field using distance constraints (FXDI) set to ±20% of the measured values (Table S4) and the angles (FXTA) constrained as described in the text. Up to 1000 iterations using the convergence method PRCG[94] were performed for each structure. After each set of iterations (300 for cyclo-[L-BTD-Ala-Trp-Arg-Tyr, 200 for cyclo[D-Pro-Phe-Ser-Trp-Arg-Tyr), the backbone atoms of each minimized structure were compared to all previous structures with the COMP command, discarding conformations that were too high in energy, as specified by the DEMX command; the threshold was set very high, at 250 kJ, initially, and then decreased in 50 kJ increments to a minimum of 100 kJ. Duplicate structures were also discarded after each set of iterations; i.e., if the rms difference between backbone atomic positions was below the threshold specified by the CRMS command; this threshold was set initially to 0.2 Å and then increased by 0.1 Å after each set of iterations to a maximum of 0.5 Å. By discarding structures at intermediate stages, the total computational time was reduced considerably. Finally, the FMNR (full matrix Newton Raphson) convergence method was used for up to 50 iterations to bring the gradient under 0.01 kJ/(Å mol). The structures were then reordered by increasing energy.

Acknowledgment. This work was supported by a grant from the National Institutes of Health (Grant No. GM30759) and a postdoctoral fellowship from the American Cancer Society (to M.A.L.). We thank Dr. Stephen Telfer for first recognizing the conformational similarity between tendamistat and cyclo[D-PFTFWF], Georges Lauri for help with the programs for calculation of distances from integrated cross-peak volumes, and Prof. R. Huber, Dr. O. Epp, and Dr. G. Wiegand (Max Planck Institut für Biochemie, Martinsried) for providing the coordinates of tendamistat and preliminary communication regarding the structure of the tendamistat−α-amylase complex. Linear hexapeptides were kindly provided by Simon Ng and Dr. Reyna Simon of Chiron Corp.

Supplementary Material Available: Text explaining the synthesis and characterization of intermediates not described above, tables, text, and figures giving NMR pulse sequences and data for structural assignment of **3**, **4**, and L-**7**, tables listing the coordinates for lowest energy structures in Figures 6−8, and programs for calculation of distances from integrated cross-peak volumes (25 pages). This material is contained in many libraries on microfiche, immediately follows this article in the microfilm version of the journal, and can be ordered from the ACS; see any current masthead page for ordering information.

(91) McCroskey, R. P. U.S. Patent 1984, 4,472,499, 18.
(92) Bodanszky, M. *Peptide Chemistry. A Practical Textbook*; Springer-Verlag: Berlin, Heidelberg, 1988.
(93) Felix v1.0, Hare Research Inc., Woodinville, WA.
(94) Polak, E.; Ribiere, G. *Rev. Fr. Inf. Rech. Oper.* **1969**, *3*, 35−43.